Hindawi
Journal of Chemistry
Volume 2023, Article ID 8730221, 36 pages
https://doi.org/10.1155/2023/8730221

Review Article

Recent Advances in Conversion of Glycerol: A Byproduct of Biodiesel Production to Glycerol Carbonate

Arpita Das,[1] **Pravin Kodgire**,[2,3] **Hu Li**,[4] **Sanjay Basumatary**,[5] **Gurunathan Baskar**,[6] **and Samuel Lalthazuala Rokhum**[1]

[1]*Department of Chemistry, National Institute of Technology Silchar, Assam 788010, Silchar, India*
[2]*Chemical Engineering Department, Pandit Deendayal Energy University, Gandhinagar 382426, Gujarat, India*
[3]*Center for Biofuel and Bioenergy Studies, Pandit Deendayal Energy University, Gandhinagar 382426, Gujarat, India*
[4]*State-Local Joint Laboratory for Comprehensive Utilization of Biomass, Center for R&D of Fine Chemicals, Guizhou University, Guiyang, Guizhou 550025, China*
[5]*Department of Chemistry, Bodoland University, Kokrajhar 783 370, BTR, Assam, India*
[6]*Department of Biotechnology, St. Joseph's College of Engineering, Chennai 600119, India*

Correspondence should be addressed to Samuel Lalthazuala Rokhum; rokhum@che.nits.ac.in

Received 1 November 2022; Revised 6 January 2023; Accepted 21 June 2023; Published 1 July 2023

Academic Editor: Vijay Kumar Garlapati

Owing to erupted ecological concerns and escalated energy consumption, biodiesel produced by transesterifying nonedible and used cooking oils has been acknowledged as a viable source of clean and sustainable energy, alternative to fossil fuels. This transesterification process led to an excessive supply of glycerol as the primary byproduct which can then be transformed into value-added derivatives, primarily glycerol carbonate (GC), thereby drawing attention to its potential use in industrial applications. Although several methods for synthesis of GC utilize glycerol as building block, the transesterification approach using dimethyl carbonate (DMC) is the most effective route implementing safer and greener reaction conditions. This review is focused on different types of heterogeneous catalysts and characterization techniques used for identifying and deactivating those catalysts, covering the literature from the last decade to till date on this topic. Potent applications of GC as a versatile compound are elucidated in brief. Finally, a conclusion, outlook, and author's perspective have been provided in brief.

1. Introduction

Global warming and asymptotic depletion of fossil fuel supplies, resulting from the dramatic population growth, have intensified the energy crisis. This has prompted the need for renewable energy sources. Biodiesel has become a widespread alternative energy source as the CO_2 emissions could be reduced by about 70% by switching to biodiesel compared to the conventional fossil fuels. Hence, biodiesel production has increased exponentially in the recent decades. Owing to this, global generation of glycerol, the main byproduct of biodiesel synthesis by transesterification of vegetable oil and animal fats, has significantly increased. The indispensable production of glycerol byproduct reduced the profitability margins of biodiesel industries, yet warranted alternative utilization of surplus byproduct glycerol, a promising opportunity to acquire value-added products from renewable raw materials.

Statistics show that between 2000 and 2020, the world's biofuel production increased at a fast pace (Figure 1) [2]. A major apprehension in biodiesel synthesis is the generation of the byproduct, glycerol, posturing an environmental issue when waste is burned or dumped directly in landfills. In this context, conversion of raw and unprocessed glycerol into the high value-added derivative glycerol carbonate (GC) and use as a fuel additive or even fuel is one potential solution to deal with overflow of crude glycerol. Esters of carbonate have been found to reduce particle emissions during engine combustion dramatically, according to previous findings. As shown in Figure 2, GC, one of the glycerol derivatives, is

synthesized via transesterification with dimethyl carbonate (DMC). This route has attracted scientific interest due to its industrial relevant properties such as elevated boiling point, poor flammability, less toxicity, biodegradability, and high cetane number. It might be noted that during GC formation from transesterification of glycerol and DMC, formation of three main side products such as glycidol, methyl ((2-oxo-1,3-dioxolan-4-yl) methyl) carbonate, and bis ((2-oxo-1,3-dioxolan-4-yl) methyl) carbonate often took place, reducing the selectivity toward GC, as shown in Figure 3. Hence, production route favouring the selective and/or exclusive production of GC remains a challenge.

Glycerol, chemically known as propane-1,2,3-triol, contains three hydroxyl (-OH) groups and a three-membered carbon backbone which attributed to its hygroscopic and hydrophilic nature. The versatility of the structure of glycerol makes it a desirable molecule for innovation in organic synthesis. The value of the worldwide glycerol market in 2019 was USD 2.6 billion [5]. In 2020, the global production of biofuel ascended to 1677 thousand barrels of oil equivalent per day in contrary to 187 thousand barrels of oil equivalent per day produced in 2000. By 2024, it is anticipated that the worldwide biofuels market will worth 153.8 billion US dollars. In addition, it is expected to rise at a compound annual growth rate (CAGR) of 4.0% between 2020 and 2027. In the chemical market, manufacturing of bio-based products has risen to prominence in the industries of lubricants, solvents, plastics, and surfactants. Over the forecast period of 2019–2027, an increase is assumed at a CAGR of 16.67% [5]. Nonetheless, every 1000 kg of biodiesel produced will generate about 100 kg of glycerol, a byproduct [6–8]. Therefore, with the widespread synthesis of biodiesel, effective glycerol recycling has become an important and highly sought-after research focus. In order to achieve efficient glycerol conversion and promote sustainability of biodiesel industry, it is necessary to create derivatives with high value-added from low-value glycerol. At present, it has been extensively employed as an initial substrate for a variety of synthetic processes, including reduction, esterification, dehydration, carbonylation, oxidation, and etherification, among others. (Figure 4).

As listed in Table 1, glycerol can be transformed into a variety of value-added derivatives that include GC, mesoxalic acid, dihydroxyacetone, mono-/di-/triglycerol ester, syngas, 1,2- propanediol, glyceric acid, glycerol 1,3-bromo- and iodohydrins, oxalic acid, hydrogen, tartronic acid, and polyglycerol mono-/di-/tri-GTBE. GC, among the numerous conversion products of glycerol, has been extensively investigated for its superior amenities. A highly versatile raw material, GC, belonging to the family of organic carbonates, is usually referred to as typical "green chemistry" products due to their distinctive advantages in various areas, such as pharmaceutical intermediates, high boiling point solvents, and material intermediates. In particular, GC has gained much attention because it has been an area of research for investigating direct implications for producing glycidol which is frequently utilized in cosmetics and paints. In addition, GC finds indirect usage in the production of polyols, polyglycerols, polycarbonates, polyurethane, and a variety of other polymers. Moreover, derivatives of glycerol carbonate such as glycerol carbonate methacrylate [40] and furanic derivatives of glycerol carbonate [41] are becoming more valuable starting materials for the production of polymers. Glycerol carbonate (GC) differentiates out among the known cyclic carbonates since it behaves as an efficient and flexible bifunctional key component in polymers and biomedical applications [42, 43]. In addition, it is used as a more effective solvent or as a membrane covered in gas separation units in the lithium-ion battery industry [44, 45]. As a consequence, generation and utilization of organic carbonates have now received enormous attention from researchers [46–48].

As a result, this review will provide an overview of several synthetic methods used to produce GC, emphasising on the process pathways, catalysts, and reaction mechanisms. In addition, it seeks to emphasize the process' potential industrial utility. The process' potential for industrial application is therefore expressly intended to be highlighted.

2. Glycerol Carbonate (GC) Production: An Overview

The primary focus of the study has been on GC synthesis which is economical as well as ecologically beneficial in preparation for industrial scale-up. As a result, new methods of producing GC are constantly developing following the growing demand for GC applications across various industries [5, 42]. The following units are dealt with the most recent advancements in the manufacturing of GC in the present scheme.

2.1. Different Synthetic Routes of GC. A direct and an indirect synthetic technique can be employed to synthesize glycerol to GC, as summarized in Figure 3. Using glycerol as source of alcohol and substances like CO/O_2, urea, CO_2 or dialkyl carbonate as carbonate sources, GC can be developed in various ways. Among all the routes for GC synthesis, one of the easiest and economically feasible methods for synthesizing high GC yields is transesterifying glycerol with dialkyl carbonate, chiefly DMC. The mechanism section will thoroughly describe the method of the synthesis [48]. GC has been produced indirectly through a widely applicable synthetic approach of phosgenation and carboxylation of glycerol. This method causes the creation of GC when carbonate and alcohol sources are used in the exchange reaction. Researchers typically use carbonate additives in the glycerol upgradation to produce GC, including CO, CO_2, urea, phosgene, ethylene carbonate, dimethyl carbonate (DMC), and diethyl carbonate (DEC) [2]. Figure 5 depicts various carbonate supplements and methods for GC production from glycerol.

However, using ecologically unfriendly reactants raises ecotoxicity concerns, creating a nuisance and generating hazardous side products that are detrimental to human health. Because of the toxicity and challenging use in chemical reactions, urea, phosgene, and CO usage are largely restricted. For instance, glycerol and urea reaction, apart

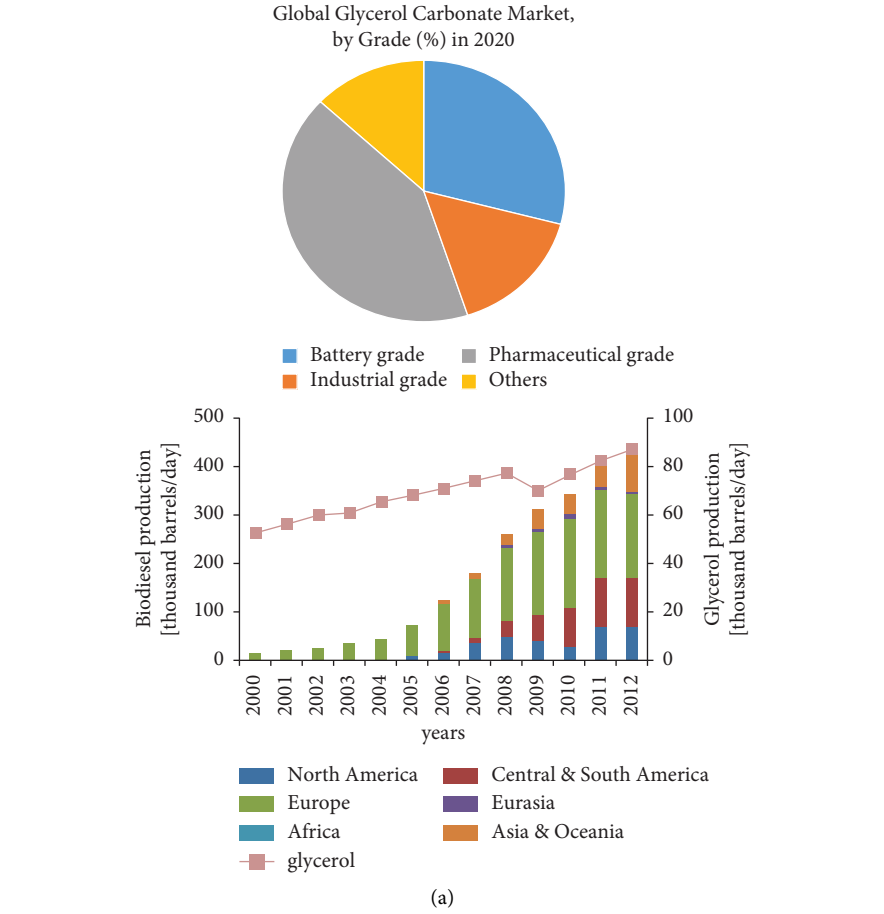

Figure 1: (a) Biodiesel and glycerol production vs. years (reproduced from [1]). (b) Graph showing increase in global biofuel production between 2000 and 2020. Source: global energy and CO_2 data.

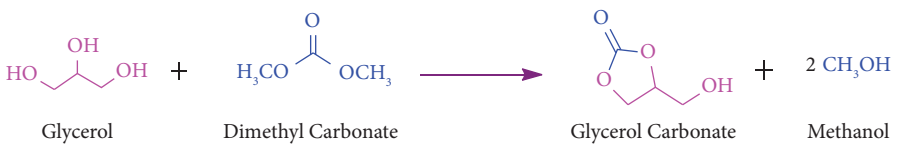

Figure 2: Synthetic scheme of GC through glycerol transesterification with DMC [3].

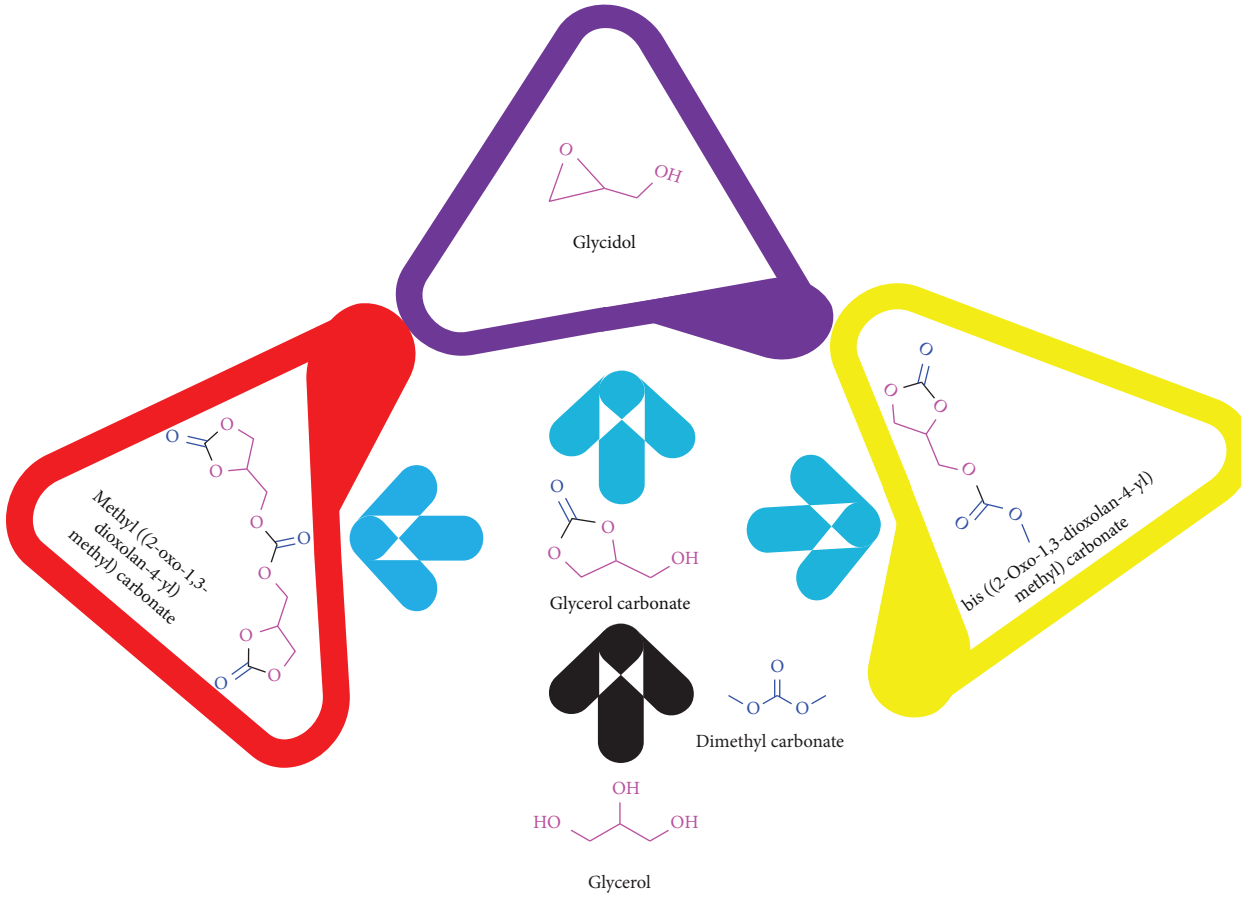

Figure 3: Glycerol carbonate production and associated side products [4].

from producing GC, produce hazardous isocyanic acid and biuret. In addition, a vacuum must be applied continuously during the whole reaction process to eliminate ammonia [49]. As a result, their application (urea) in glycerolysis has been widely overlooked. Accordingly, utilizing cleaner and nonhazardous processes to handle chemicals is chosen for the green synthesis of GC.

2.2. GC Production through Transesterification. The most promising, efficient, and economically feasible method for producing GC is the transesterification of glycerol using DMC [50]. Even though glycerol is thermally stable, it needs maximum threshold energy for breakage of bond and to participate in the transesterification reaction. Therefore, the effective catalyst applied, which can suggest an eventual lower-activation-energy reaction pathway, is the key criterion to ensure a feasible glycerol transesterification. However, the utilization of DMC in the catalytic GC synthesis has been discovered as a sustainable route as it reduces the energy needed for glycerol conversion and boosts the GC yield. Like heterogeneous and homogeneous catalysts, enzymes as biocatalysts also play a vital role in glycerol transesterification. Numerous reports on this type of catalytic transesterification using a broad range of catalysts with various property combinations have been published [49, 51]. The catalytic activity of both homogeneous and heterogeneous acidic catalysts has been reported to be quite low, hence not suitable for GC synthesis [44]. Although homogeneous catalysts exhibit greater activity, there are drawbacks such as nonrecyclability, difficulty, and time-consuming separation of products. Although it has been found that enzyme catalysts are preferable, they cannot be reused and denatured under vigorous reaction conditions. Because of the fast phase separation ability from reaction products, heterogeneous catalysts are considered as the most significant catalyst for transesterification of reactions. It generates GC through glycerol valorization as they are easily separable from the products and reusable providing cost-effectiveness. Among heterogeneous catalysts, base catalysts are preferable to acid catalysts because they are less abrasive, safer, and ecofriendly. All these different catalysts are elaborated further in Section 4.

In order to produce GC from glycerol, a range of inorganic and organic catalysts are used, including enzymes [51], ionic liquids, hydrotalcites [52], mixed metal oxides [53, 54], metal supported on metal oxide [55, 56], and zeolites. In the meantime, as utilizing biomass waste as a catalyst source addresses the problem associated with waste disposal and controls the GC production economy through transesterification, researchers have become much more concerned about the utilization of catalysts derived from

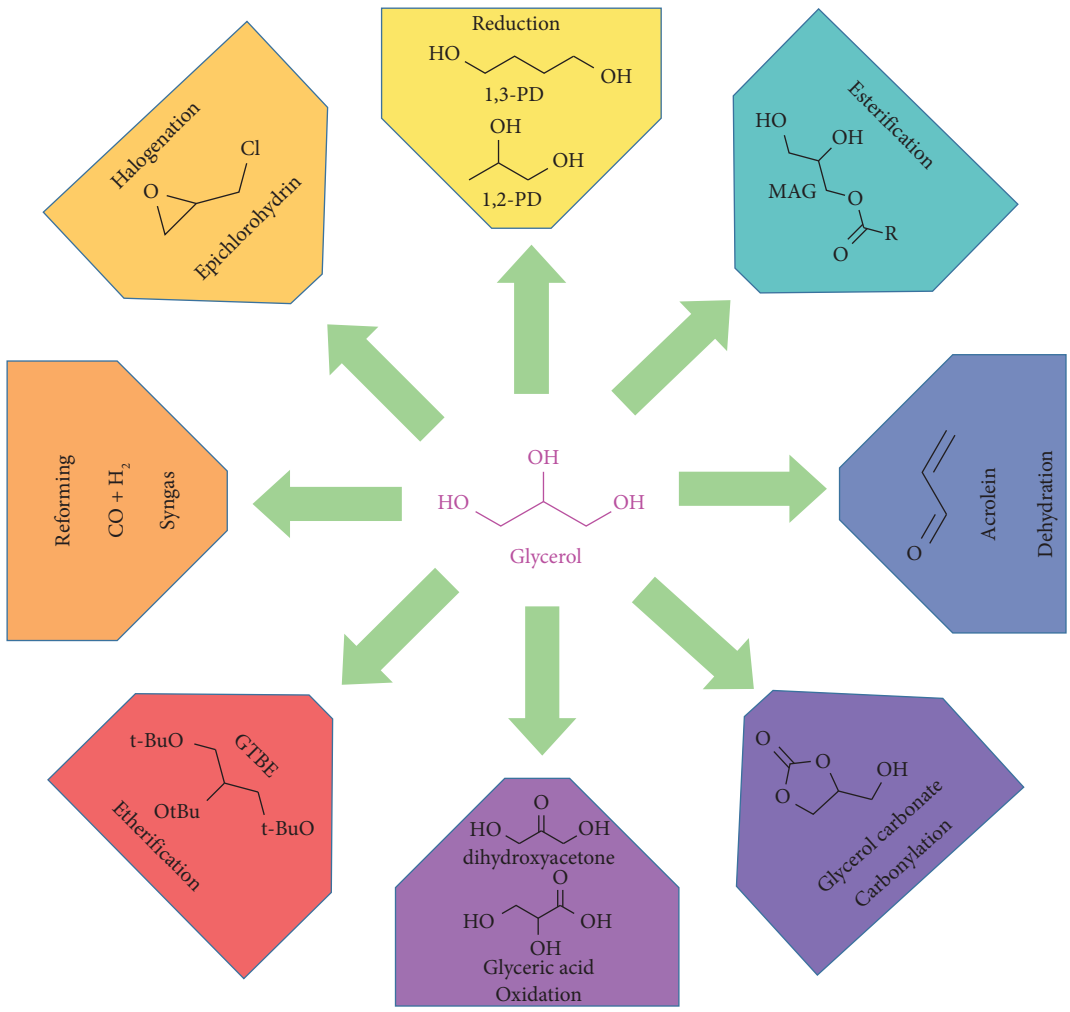

Figure 4: Synthesis of high value-added chemicals obtained from glycerol valorization (adapted from [9]).

biowaste (Table 2) [57, 58] for GC synthesis. The effectiveness of the basic catalyst prepared from *Musa acuminata* peel ash (MAPA) for GC production was reported by Changmai et al. [59], and recently, Das et al. [60] utilized *Mangifera indica* peel ash (MIPCA) catalyst for microwave-assisted glycerol transesterification. The catalysts derived from biomass waste MAPA comprised of CaO (7.78%), MgO (2.42%), and SiO_2 (10.86%), with K_2O (the primary active component) conjuring up 65.9% of the total composition. Similarly, MIPCA comprised of SiO_2 (15.42%), CaO (26.2%), MgO (8.53%), and the primary active component K_2O (37.9%) responsible for appreciable high basicity. Under microwave irradiation, MAPA showed 99% conversion of glycerol and high GC selectivity of 99.5%, while MIPCA exhibited glycerol conversion and GC selectivity of 98.1% and 100%, respectively, under optimized reaction conditions (Table 2, entries 8 and 9). A thorough discussion of the use of catalysts for GC production in the transesterification reaction utilizing DMC is provided in the subsequent sections.

3. Mechanism of Glycerol Transesterification with DMC to GC

After a thorough review process, it is found that glycerol transesterification with DMC for GC production is controlled by a number of variables that include catalyst concentration, temperature, molar ratio, duration, and supply of energy [70]. To enhance the production of GC and its selectivity, fully comprehending these parameters impact on glycerol conversion is crucial. Numerous researchers have proposed hypothesized reaction routes using DMC and glycerol reactant molecules.

The reaction steps are briefly described as follows [9] (Figure 6):

(1) On the top of catalyst's surface, both glycerol and dimethyl carbonate get adsorbed. Glyceroxide ($C_3H_7O_3^-$) anion is generated as a result of glycerol's intermolecular absorption into the surface of the

Table 1: Value-added derivatives of glycerol and their synthesis with various enzymes and chemical catalysts.

Reactions	Reactants	Catalysts	Products	Reference
Condensation	Acetone	Solid SnF_2	2,2-Dimethyl-1,3-dioxolane-4-methanol	[10]
	Formaldehyde	H_2SO_4		[11]
		Propyl sulfonic acid functionalized SBA-15 and KIT-6	1,3-Dioxolane-5-ol and 1,3-dioxolane-4-methanol	[12]
Dehydration	Glycerol	WO_3/ZrO_2@Si	Acrolein	[13]
		Phosphotungstic acid ($H_3PW_{12}O_{40}$) catalyst supported on CARIACT-Q10 commercial silica		[14]
		PO_4/Nb_2O_5		[15]
		Nanosheet MFI zeolites		[16]
		H-ZSM-5		[17]
		Iron phosphate		[18]
Etherification	Ethyl alcohol	H-Beta and USY-650-L-2 zeolites	Glycerol ethyl ether	[19]
	tert-Butyl alcohol	Zeolite	Polyglycerol mono-GTBE di-GTBE tri-GTBE	[20]
	—	Waste egg shells	Glycerol oligomers	[21]
	TBA	TTBG	Sulfonic acid silica-based catalyst	[22]
Esterification	Lauric acid	Arene sulfonic acid functionalized alkyl bridged organosilica	Monoglycerol ester Diglycerol ester Triglycerol ester	[23]
	Acetic acid	Lipase from *Candida* sp.		[24]
Halogenation	Glycerol	1. Glycerol-1,3-dichlorohydrin through multigrams via Conant's methodology 2. Bromo and glycerol iodohydrins via Finkelstein's reaction using NaI, NaBr salts, and organic additives (TBAI and TBAB)	Glycerol 1,3-bromo and iodohydrins	[25]
Pyrolysis		$LaNi/\alpha\text{-}Al_2O_3$	Syngas	[26]
	Oxidative steam	Co/Al coprecipitated catalyst		[27]
Selective oxidation	Selective oxidation of glycerol	Laccase/2,2,6,6-tetramethylpiperidine-N-oxyl system	Mesoxalic acid	[28]
	Selective photo electrochemical oxidation of glycerol	Nanoporous $BiVO_4$ photoanode	Dihydroxyacetone	[29]
	Selective electrochemical conversion	Amberlyst-15 over Pt/CBAC (mixed carbon-black activated carbon) electrode	Glycolic and lactic acid	[30]
Selective reduction	Fermentation of soyabean cake hydrolysate	*Citrobacter freundii* strains	1,3-Propanediol	[31]
	Metabolic pathway	*Pseudomonas denitrificans*		[32]
	Hydrogen + glycerol	Ru-Co/ZrO_2	1,2-Propanediol + ethylene + glycol	[33]
	NADH-generating glycerol catabolic pathway	*Saccharomyces cerevisiae*	1,2-Propanediol	[34]
	Hydrogen	Nb-modified Pd–Zr–Al		[35]
	Hydrogen	Ni-Cu catalysts supported on Y-zeolite		[36]
	Hydrogen	Cu-Zn hydrotalcites		[37]
	In situ hydrogen production	$Cu/ZnO/Al_2O_3$		[38]
Cycloaddition	Glycidol + CO_2	TBD@Merrifield	Glycerol carbonate	[39]

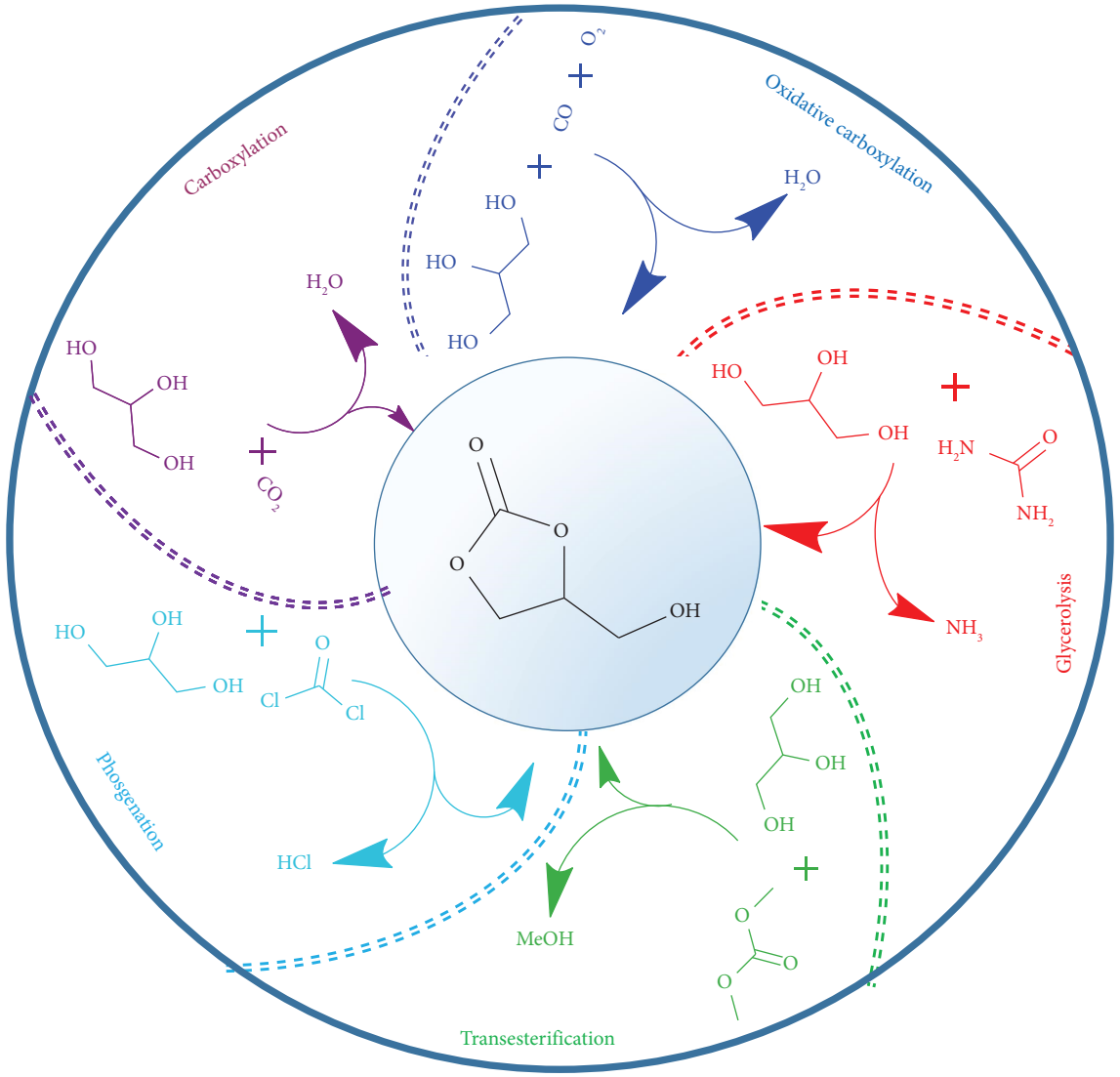

Figure 5: Direct and indirect synthetic routes to glycerol carbonate [9].

catalyst, which occurs when the O-H bond in glycerol is cleaved by abstraction of hydrogen.

(2) Afterwards, glyceroxide anion proceeds in close vicinity to dimethyl carbonate that has been adsorbed. The nucleophilic attack happens between glyceroxide ion and dimethyl carbonate which results in the formation of methyl glyceryl carbonate and a methoxide ion.

(3) By abstracting one H^+ ion from the catalyst surface (which was previously abstracted by the catalyst from glycerol), methoxide ion produces methanol. Furthermore, the oxygen anion group is then left in glycerol when catalyst's active basic site removes another H^+ ion from the secondary hydroxyl group. After 2nd nucleophilic attack on the carbonyl carbon, this glycerol anion oxygen undergoes a cyclization reaction, which removes a further methanol group to generate GC.

However, in the presence of a highly basic catalyst or in higher temperature, GC undergoes decarboxylation reaction forming glycidol, as shown in Figure 7. This glycidol can further be transformed to GC by cycloaddition of CO_2 to glycidol, an atom-economic efficient strategy that can be accomplished under mild reaction conditions using very simple or even bio-based catalysts [39, 71].

4. Catalytic Production of GC

4.1. Homogeneous Catalyst. Homogeneous catalysts comprised of bicarbonates, alkoxides, potassium or sodium carbonates, organic ILs, and hydroxides are widely reported for manufacturing GC utilizing DMC. The catalytic performance of acid catalysts during transesterification has been recognised to be incredibly low. While basic catalysts produce a higher glycerol conversion with increased selectivity, acid catalysts are abrasive and fragile in the reaction mixture. Hence, basic catalysts [72–75] are usually employed

Table 2: Waste material and biomass-derived catalysts.

Sl. No.	Heterogeneous catalyst	Reaction conditions[a]	Conversion	Selectivity	Yield	Reaction cycles	References
1	Disposable baby diapers waste-derived catalyst	1 : 4, 75, 1, 2	95.6	—	93.6	8	[57]
2	Waste red mud (active $NaAlO_2$ and Ca_2SiO_4)	1 : 3, 75, 1.5 h, 12.5	95.2	—	92	4	[61]
3	Waste carbide slag	1 : 5, 75, 1.5, 3	98.1	—	96		[62]
4	CaO from natural sources (egg shell, golden apple snail shells, and cockle shells)	1 : 3, 80, 2, 3	—	—	92.1	—	[63]
5	Porous biochar derived from pyrolysis of fishery waste	1 : 2, 85, 1, 2	100	—	99.5	5	[64]
6	Waste crayfish shell	1 : 6, 75, 1.5, 4	98.7	—	95.3	3	[65]
7	*K*-zeolites derived from coal fly ash	1 : 3, 75, 1.5, 4	100	—	96	4	[66]
8	Calcined *Mangifera indica* peel ash catalyst	1 : 3, 80, 50 min, 6	98.1	100	—	5	[60]
9	*Musa acuminata* peel ash catalyst	1 : 2, 75, 15 min, 6	99	99.5	—	6	[59]
10	Oil palm empty fruit bunch ash catalyst	1 : 3, 90, 45 min, 5	—	—	95.7	4	[67]
11	Palm fuel ash-derived catalyst	1 : 5, 80, 112 min, 5	97	—	90	5	[58]
12	Corncob residue-derived catalyst	1 : 3, 80, 1.5, 3	98.1	—	94.1	3	[68]
13	Rice husk-derived catalyst	1 : 4, 70, 2.5 h, 4	98	—	92	4	[69]

[a]Glycerol: DMC molar ratio, temperature (°C), reaction time (h), and catalyst loading (wt.% w.r.t glycerol mass). Note: "—" is not discussed.

for the production of GC (Table 3). To seek the minimal operational circumstances possible in fulfilment of sustainable development is one of the principal goal of implementing the "green processes" [78]. Under mild operating circumstances, Esteban et.al. [72] conducted glycerol transesterification with (a) DMC and (b) ethylene carbonate (EC), utilizing CH_3OK as a homogeneous catalyst. It was observed to coproduce valuable CH_3OH and ethylene glycol, respectively, with GC as the major product. This catalyst was almost entirely selective towards the desired product GC in both the cases. In a different study, Esteban et al. [79] employed K_2CO_3 as a catalyst to transesterify glycerol with DMC and EC, and under ideal reaction conditions, 99.27% glycerol conversion was obtained with DMC as precursor. It was observed that employing CH_3OK could greatly improve the interval's ability to function using K_2CO_3. Its activity significantly reduced below 66°C likely because of solubilization concerns below this temperature. For reaction with EC, two further tests were carried out using K_2CO_3 as a catalyst at 313 and 323 K; the minimum and maximum temperatures in previously assessed range were evaluated along with the kinetic investigations conducted with CH_3OK to develop a model of kinetics. Even while performing at lower temperatures, the reaction using EC acquired substantially greater turnover frequency (TOF) values compared to reaction DMC. When comparing each individual reaction with DMC, it can be shown that using CH_3OK at 66°C (runs 1 and 2), TOF raised by up to 19.89 times and at 70°C (runs 3 and 4) by 17.31 times. At 40°C (runs 7 and 8) and 50°C (runs 9 and 10), the TOF increased by 6.57 and 5.36, respectively, showing that the application of CH_3OK in the reaction using EC also improved performance, although not as much as in the other reaction. Lastly, the effectiveness of CH_3OK was demonstrated by comparison to K_2CO_3, demonstrating its superior activity.

N-Heterocyclic carbene (NHC) has long been employed as an active organic base catalyst by Hervert et al. [73] and as an effective homogeneous organocatalyst for glycerol transesterification. Considering the ease of catalyst recovery and reusability, Hervert et al. [73] immobilised NHC on mesostructured cellular foam supported on silica with a protecting group of hydrogen carbonate. The glycerol transesterification (Figure 8) strategy functioned smoothly with the assistance of this "masked" NHC precatalyst with a yield of 75% and a GC selectivity of 91%. It was easily recoverable and reusable up to the 3rd cycle. These organic strategies provide an innovative and convenient access to GC from glycerol using a heterogenized masked organic base which also serves as a source of concepts for numerous organocatalyst for transesterification.

4.2. Heterogeneous Catalyst. A survey of the literature revealed that catalyst separation from the reaction system is a great concern for alkali or alkaline hydroxides [3, 75] and carbonate [74–76] homogeneous catalysts, which limit their use from an industrial perspective. Due to the laborious and expensive separation processes required to separate homogeneous catalysts from reaction products, utilization of homogeneous catalysts is preferentially unacceptable despite the high cost of overall biodiesel production.

To overcome the restrictions correlated with the usage of homogeneous catalysts, researchers began examining the effectiveness of heterogeneous catalysts. Findings have revealed that the most effective catalysts for glycerol transesterification to GC are heterogeneous bases because of their basic strength and stable interphasic mass transfer. According to reports, inorganic bases have potent basic active sites that can accomplish glycerol moiety's deprotonation to carry out further activities that build and break bonds during the transesterification reaction. The maximum catalytic activity is found in alkali/alkaline metal oxides because of their strong basic nature, which ultimately causes glycerolysis during transesterification. In addition, the most sought-after catalysts include metal supported on metal oxides, mixed oxides, hydrotalcite from mixed metal oxides, basic zeolites, nanocatalysts, ionic liquids, and enzymes as biocatalysts discussed elaborately with examples in the following section.

4.2.1. Metal Supported on Metal Oxide. Solid catalysts', which usually comprise several components, interfacial interactions have been documented as an important factor influencing architectures and catalytic performance. Strong metal-support interactions (SMSI) and electronic metal-support interactions (EMSI) are two crucial concepts that have been thoroughly recognised and their effects on metal catalysis have been adequately illustrated in the context of oxide-supported metal catalysts (metal/oxide catalysts). Herein, we present a thorough assessment of the developments in the MSI of metal/oxide catalysts.

Song et al. [81] synthesized GC utilizing an efficient and economic Li/ZnO catalyst, developed by infusing ZnO in $LiNO_3$ solution (Figure 9). It was demonstrated that the catalysts' basicity was profoundly affected by Li dosage and calcination temperature. The straining of Zn-O bonds caused by replacement of Zn^{2+} in ZnO lattice by Li^+ and the generated (Li^+ O^-) species hence catalysed transesterification. ZnO loaded with 1 wt.% lithium nitrate and 500°C calcination temperature displayed the maximum catalytic activity. Conversion of glycerol (97.40%) and yield of GC (95.84%) were obtained under optimal conditions over this catalyst.

Utilizing the wet impregnation method, Jaiswal et al. [55] developed an extremely efficient heterogeneous catalyst, Li/TiO_2 and transesterified glycerol with DMC to produce GC. According to studies, the calcination temperature modifies the composition and the acidic and basic properties of mixed metal oxides. A Hammett indicator analysis was performed to examine overall basicity of active sites of the prepared catalyst. The basic strength lies in the range of $15 < H < 18.4$ when the Li concentration is increased from 5 to 25 wt.%, and 25 wt.% Li/TiO_2 has basicity of 19.54 mmol·g^{-1}. In addition, $(Li_2TiO_3)_{10.66}$ crystals, having mean particle size of 49.39 nm, are formed when the Li concentration is increased to 25 wt.% of TiO_2, indicating the produced catalyst as a nanocatalyst. The catalyst's morphology remained constant

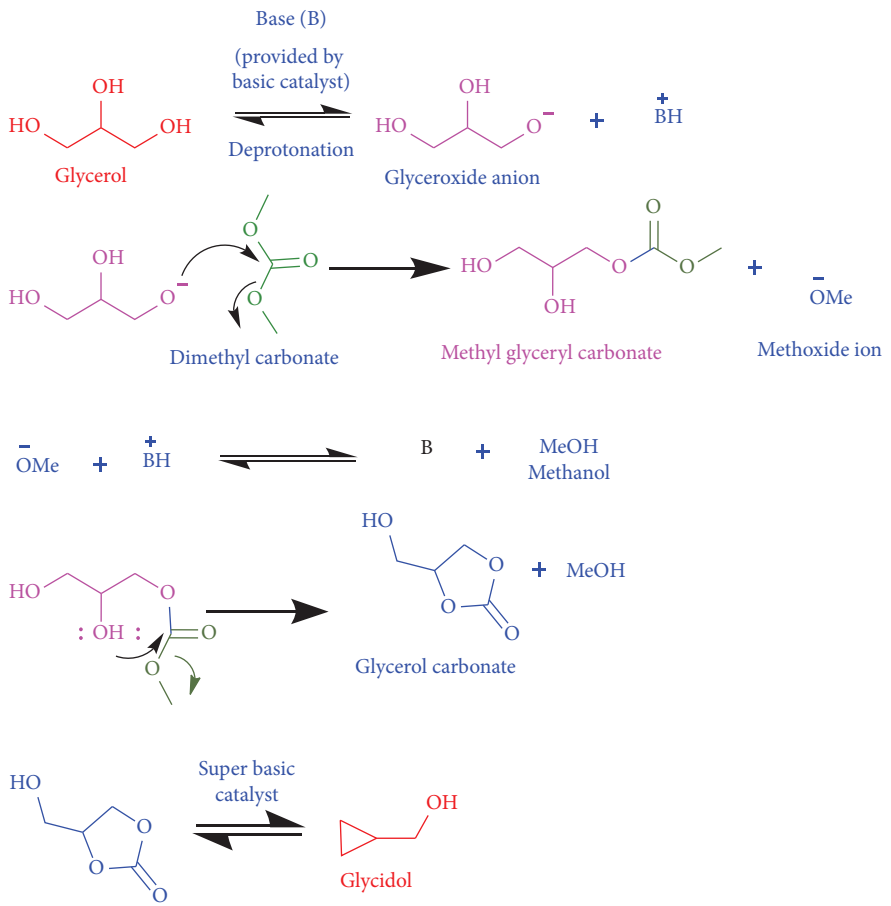

Figure 6: Plausible mechanism for the synthesis of GC from glycerol (reproduced from [60]).

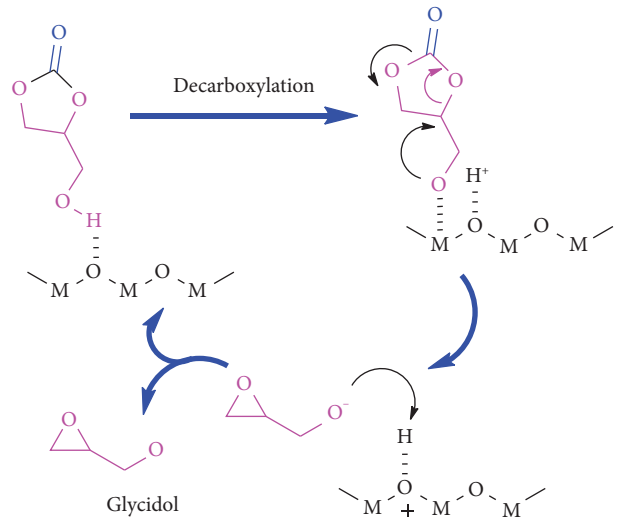

Figure 7: Pictorial representation of glycidol formation reaction in the presence of highly basic catalyst (adapted from [2]).

after five cycles, demonstrating its stability during the reaction. On titania-based catalysts, various alkaline metals including Li/g-Al_2O_3, Li/ZrO_2, and Li/TiO_2 are incorporated and were developed based on their basic strength. Li/TiO_2 displayed the most promising outcome with glycerol conversion (95.5%) and GC selectivity (95.9%), respectively, under optimum conditions (3 : 1 M ratio of DMC to glycerol, 90°C, 2 h, 5 wt.%).

With different Li contents, Li et al. [82] examined a class of Li-La_2O_3 catalysts (varying amounts of Li from 0.74%

Table 3: Homogeneous catalyst.

Sl. No.	Homogeneous catalysts	Reaction conditions[a]	Selectivity	Yield	References
1	K_2CO_3	1 : 3, 80, 1.5, 4	90	85	[74]
2	K_2CO_3	1 : 4, 90, 1.5	89	86	[76]
3	K_2CO_3	1 : 3, 25, 1.5, 4	—	82	[75]
4	KOH	1 : 3, 85, 3, 3.22	—	85.85	[75]
5	NaOH	1 : 1, 65, 1, 3	94	82	[75]
6	Triethylamine	1 : 5, 87.5, 4	—	89	[77]
7	*N*-Heterocyclic carbenes	1 : 4, RT, 20 min, 4	92	—	[73]

[a]Glycerol: DMC molar ratio, temperature (°C), reaction time (h), and catalyst loading. Note: "—" is not discussed.

Li_2O to 3.50% Li_2O) under mild reaction conditions for GC synthesis via transesterification. Li doping into La_2O_3 influenced the growth of the crystal phase of La_2O_3, causing La_2O_3's (002) crystal plane's lattice to grow; as doped, Li might penetrate the La_2O_3 lattice and also increase the catalytic performance of Li-La_2O_3 for GC selectivity and yield. Adding Li into La2O3 also boosted the impact and measure of basic sites of the 3.50 Li-La_2O_3 catalyst thereby increasing catalytic activity and interaction between Li and La_2O_3. The 3.50Li-La_2O_3 sample exhibited the maximum binding energy shifts, and the XRD characterization illustrated the comparatively strong interaction between lanthanum and lithium. Moreover, 600°C was chosen as calcination temperature as 3.50Li-La_2O_3-600 had the highest glycerol conversion and GC selectivity among the catalysts (400–700°C).

Employing wet impregnation approach, Pradhan and Sharma [56] devised a heterogeneous Mg/ZnO base catalyst (Figure 10) throughout 2 h at 80°C with 1 : 4 glycerol: DMC molar ratio. Compared to previously developed catalysts (Ba/ZnO, Sr/ZnO, K/ZnO, and Mg/ZrO_2) at the same reaction conditions, 3 wt.% Mg-doped ZnO produced the highest conversion of glycerol (98.4%), GC yield (96.57%), and selectivity (98.37%). In addition, when the calcination temperature rises, the catalyst's basicity increases, facilitating GC production. However, it was found that glycerol conversion was the highest when Mg/ZnO was calcined at 550°C due to the development of potent basic sites, whilst 3 wt.% Mg/ZnO calcined at 750°C results in less glycerol conversion and GC yield because of extremely high basicity, thereby, resulting in the decarbonylation of GC to glycidol. Since Mg is more affordable and accessible than Sr and Ba and provides the maximum conversion and yield, Mg/ZnO was chosen as the most efficacious catalyst for glycerol transesterification.

4.2.2. Mixed Oxides and Mixed Metal Oxide. The transesterification reaction to synthesize GC is reported to offer significant potential for heterogeneous catalysis using mixed oxide catalysts, and interest in this field is escalating (Table 4). The strong and high basic sites' density in the mixed oxide catalysts resulted in remarkable catalytic activity. In terms of activity, mixed oxides outperform single metal oxide. Metals' ratio, calcination temperatures, and precipitating agents affect the catalytic activity of the mixed oxides. Typically, catalysts with variable molar ratio are developed by coprecipitation, which is then followed by breakdown and calcination at various temperatures [80].

A successful GC synthesis was demonstrated using a KNO_3-modified CaO catalyst. Hu et al. [83] prepared a variety of heterogeneous KNO_3/CaO catalysts, varying KNO_3 dosage for GC synthesis. To thoroughly examine the calcination temperature effect on catalytic performance, catalyst with 15.0 wt.% KNO_3 concentration was calcined at temperatures between 500°C and 900°C. On rising the calcination temperature from 500°C to 900°C, GC yield rose from approx. 79 to 89%. Catalysts calcined at temperatures over 600°C typically exhibit greater stability. More specifically, these catalysts' stabilities increase in the following manner: Several groups reported that the transesterification of glycerol was catalysed by alkali metal-modified mixed oxides (Table 4, entries KNO_3/CaO (15%, 500) < (15%, 600) < (15%, 900) < (15%, 800) < (15%, 700). Recycling experiments revealed that recovered KNO_3/CaO (15%, 700), 94.95% glycerol conversion, and 89.63% GC yield were acquired in the fifth cycle, significantly greater than that of unmodified CaO (15.23%). Furthermore, it has been discovered that KNO_3/CaO (15%, 700) catalyst has better water resistance than CaO.

Several groups reported that the transesterification of glycerol was catalysed by alkali metal-modified mixed oxides (Table 4, entries 4–15). Although alkali oxides are unstable, they possess powerful basic sites that can start reacting by extracting a proton from glycerol. $Mg_4AlO_{5.5}$ mixed oxides adapted by introducing $LiNO_3$, i.e., $LiNO_3$/$Mg_4AlO_{5.5}$ was utilized as an effective catalyst by Liu et al. [84] for the synthesis of GC. In addition, to form $LiAlO_2$, aluminium ions were evenly distributed throughout the MgO lattice. Complete conversion of glycerol and 96.28% GC yield were attained at 80°C for 1.5 h. $LiNO_3$ was quickly transformed into $LiAlO_2$ over $Mg_4AlO_{5.5}$ oxides, creating new strong basic sites. $Mg_4AlO_{5.5}$ possessed an *H* value of $9.8 < H < 15.0$, whereas after loading $LiNO_3$, basic strength of Li/$Mg_4AlO_{5.5}$ was enhanced to $15 < H < 18.4$. Therefore, it might be concluded that increased basic strength might enhance glycerol conversion but degrade GC selectivity.

Both MgO and CaO exhibited profound catalytic activity in glycerol transesterification with dialkyl carbonate. The Hameed group calcined dolomite, a mineral composed of $MgCa(CO_3)_2$, to produce a CaO-MgO catalyst for transesterification. Calcined dolomite investigated by Algoufi

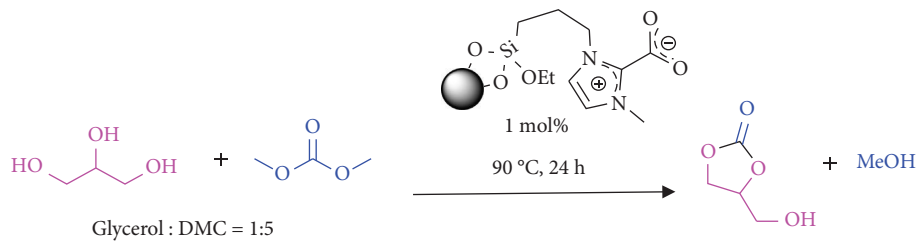

Figure 8: NHC-catalysed transesterification of glycerol (adapted from [80]).

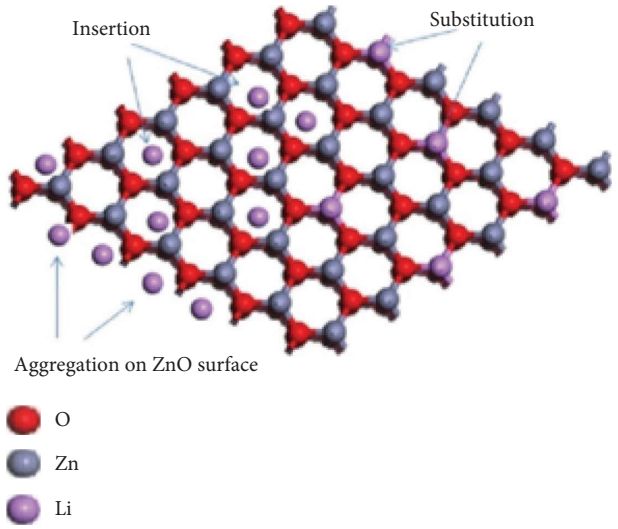

Figure 9: Li atoms are incorporated into the ZnO structure (reproduced from [81]).

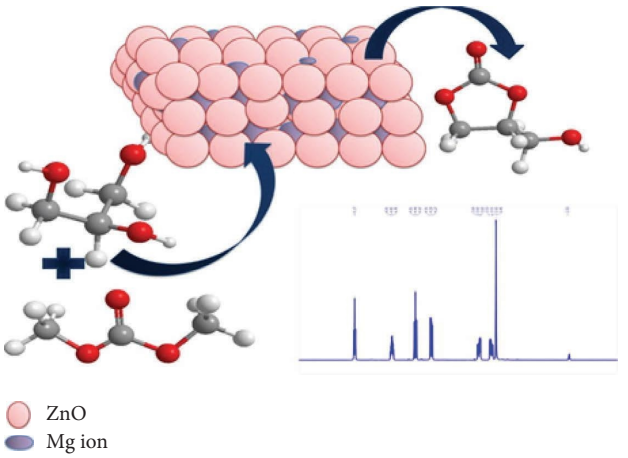

Figure 10: Mg/ZnO as catalyst for glycerol carbonate production (reproduced from [56]).

et al. [85] demonstrated the ability to catalyse glycerol transesterification for a consecutive cycle carried out under optimal condition (1 : 3 molar ratio glycerol to DMC, 75°C, 1.5 h, and 6 wt.% catalyst loading). Upon calcination at temperature 800°C, natural dolomite transformed into CaO-MgO mixed oxide, which produces the basicity necessary for converting glycerol to GC. The pores on the catalysts for the MgO and CaO phases are reduced due to rise in temperature of calcination to 900°C. This restricts the reactants' accessibility to adequate active sites and reduces the GC yield. After four reaction cycles, catalyst sustained about 84% conversion of glycerol and yield of GC around 79%.

For the transesterification of glycerol, mixed oxides of alkaline-earth metals and transition metals with modest to better yields were developed (Table 4, entries 14–16). Despite having powerful basic sites, low surface areas of lanthanide metal oxides caused declination in catalytic efficacy for transesterifying glycerol (Table 4, entries 12 and 13) [99]. Other metal oxides usually support lanthanide metal oxides to boost their surface area and catalytic performance. The GC synthesis was also investigated using CeO_2, one among the inner transition metal oxides.

Later, Parameswaram et al. [53] explored MgO-CeO_2 catalysts for the selective preparation of GC at optimal conditions (5 : 1 DMC to glycerol molar ratio, 90°C, 90 min, and 0.3 g catalyst). The highest activity was demonstrated by a catalyst with 3 : 1 MgO to CeO_2 molar ratio. Because MgO is crystalline, basicity mostly caused by MgO dispersion gets decreased. The lack of well-dispersed MgO may be the reason that the catalyst treated at 750°C has less activity. A considerable enhancement in glycerol conversion from 46% to 86% was observed with increased temperature of calcination (450–750°C) where GC selectivity was 100%.

Employing the coprecipitation technique, Wu et al. [54] developed a series of $Ce_{1-x}Cd_xO$ mixed oxide catalysts (Figure 11) for glycerol transesterifying with diethyl carbonate (DEC). Glycerol conversion rises to its maximum with increased Cd concentration in $Ce_{1-x}Cd_xO$ catalysts ($x = 0.3$), then decreases, which may be accounted for the decline in the surface area with rising temperature by the disruption of the porous structure of the mixed-metal oxides. It is interesting to note that the selectivity GC trend remained unchanged irrespective of calcination temperature. The most prevalent catalytic activity was found in $Ce_{0.7}Cd_{0.3}O$ that had been subjected to 500°C. Under the ideal circumstances (5 wt.% catalyst w.r.t glycerol, 90°C, 3 h, 3 : 1 M ratio of DEC to glycerol), 100% GC selectivity and 96.84% glycerol conversion were attained over this catalyst. In addition, adequate and strong basic sites synergistically accelerated GC conversion. Nevertheless, the catalyst's activity increased after four cycles of treatment at 500°C for five hours.

Mixed oxides such $Ce_{0.7}Cd_{0.3}O$, Ce-Ni, and MgO-CeO_2 displayed fair to exceptional catalytic performance in GC production [53, 54] when Ce^{4+} was doped into the CdO, or Ni lattice greater quantities of oxygen atoms were adsorbed

Table 4: Metal oxides as heterogeneous catalysts.

Sl. No.	Heterogeneous catalysts	Reaction conditions[a]	Conversion	Selectivity	Yield	Reaction cycles	References
1	Li/ZnO	1 : 3, 95, 4, 0.01 g	92.1	—	89	3	[81]
2	3.5Li-La_2O_3	1 : 3, 85, 3, 3.22	94.4	92.1	—	4	[82]
3	Li/TiO_2	1 : 3, 90, 2, 5	95.5	95.9	—	5	[55]
4	Mg/ZnO	1 : 4, 80, 2, 3	98.4	96.89	90.06	6	[56]
5	KNO_3/CaO	1 : 3, 70, 2, 15	99.23	85.85	85.19	5	[83]
6	$LiNO_3/Mg_4AlO_{5.5}$	1 : 3, 80, 1.5, 4	100	96.28	96.28	—	[84]
7	CeO_2-CdO	1 : 3, 90, 3, 5	96.84	100	—	4	[54]
8	MgO-CaO derived from dolomite	1 : 3, 75, 1.5, 6	97	—	94	4	[85]
9	MgO-CeO_2	1 : 5, 90, 1.5, 0.3 g		—	86		[53]
10	MgNiOx	1 : 4, 90, 1.5	97	—	82	6	[86]
11	Sr-Al mixed oxide	1 : 2, 70, 1, 3	99.4	—	100	5	[87]
12	Cu-based mixed oxide catalyst	1 : 5, 90, 1.5, 0.3 g	96.4		91.2	5	[88]
13	Ca/La mixed oxide	1 : 5, 90, 1.5, 0.217 g	94		74	4	[89]
14	Fe/La mixed oxide	1 : 5 , 240	—	100	71	—	[90]
15	S-CaMgAl MO	1 : 3, 75, 1.5 h, 3	98.3	—	90	5	[91]
16	LiCl/CaO	1 : 1, 65, 1, 3	—	—	94.19	5	[92]
17	Hydrotalcites promoted by $NaAlO_2$	1 : 2, 90, 0.5, 3	93	—	100	3	[52]
18	Ca-Al hydrocalumite	1 : 3, 70, 3, 0.15 g	93	97	—	6	[93]
19	Calcined Ca/Al LDH	1 : 3.5, 90, 3, 0.15 g	98	82	—	4	[94]
20	$NaAlO_2$	1 : 3, 90, 1, 10	—	—	96	4	[95]
21	$NaAlO_2$/CaO	1 : 4. 70, 3, 30		100	90.5	5	[96]
22	$NaTiO_2$	1 : 2, 90, 1.5, 3	98.5	96.4	94.5	5	[97]
23	Li Mg composites	1 : 3, 80, 2, 4	92.05	90.61	98.44	4	[98]

[a]Glycerol: DMC molar ratio, temperature (°C), reaction time (h), and catalyst loading (wt.% w.r.t glycerol mass). Note: "—" is not discussed.

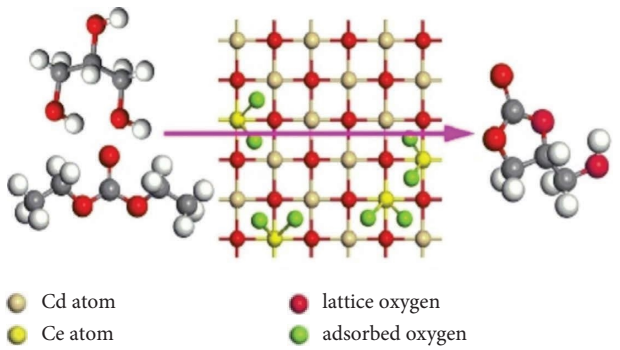

Figure 11: Synthesis of GC over CeO_2-CdO catalyst (reproduced from [54]).

on the catalyst surface which increased catalyst's reactivity. A new postulated reaction pathway was developed, as shown in Figure 12, for the transesterification. The greater number of acidic and basic sites in mixed oxides than in individual metal oxides is believed to be the reason for their enhanced catalytic activity. Two activation methods were used to promote transesterification. First, to improve the nucleophilicity of glycerol, $BaCeO_3$ phase (O^-, the Lewis basic site) of Ba-Ce catalyst removes protons from the primary hydroxyl group. The desired product, GC, was then obtained by concurrently activating carbonyl carbon of dimethyl carbonate via the Lewis acid centre (Ce^{4+}) followed by nucleophilic substitution within the molecules.

Fe-La mixed oxide catalysts, synthesized by coprecipitation technique, were reported by Pattanaik et al. [90] for GC production. The yield of this transesterification reaction is significantly lower (71%) than the aforementioned reports. The increased activity was induced by the catalyst's equimolar La_2O_3 and Fe_2O_3 composition. The catalyst produced at 550°C calcination temperature offers the highest yield, whereas dropped to 61% when temperature was raised further to 650°C.

Magnesium nickel-based mixed oxide (MgNiOx), a low-cost heterogeneous basic catalyst, was synthesized by Pradhan and Chandra Sharma [86] for GC production. E-factor, a simple ratio of amount of waste produced during the process to mass the intended product, was used to assess the transesterification process by employing 3 : 1 MgNiOx as a catalyst. When the molar ratio of magnesium content grew, the catalyst's Raman spectra show that the Raman band sharpened and altered to particular values due to Mg^{2+} integration with Ni^{2+} and the production of a solid solution of NiMg mixed oxide. The high turnover frequency and low E-factor (0.074) implied the effectiveness and environmentally benign nature.

In addition, LiCl/CaO, a highly effective heterogeneous CaO-based catalyst, was developed by Tang et al. [92] by impregnating CaO with chloride salts for the GC synthesis. LiCl/CaO displayed a noteworthy catalytic behaviour under ideal circumstances (1 : 1 glycerol to DMC molar ratio, 65°C, 1 h, 3 wt.% catalyst loading). From 400 to 600°C, the calcination temperature boosts the catalytic performance, as shown by well-dispersed CaO at this temperature. However, there is a dramatic decline when the catalyst was calcined over 700°C, as shown by the XRD result. The Li_2O_2 species, a powerful basic site formed when Li + replaces the Ca^{2+} in the CaO lattice, has significant transesterification efficiency. The yield of GC increases from 60% to 89.5% when the LiCl loading amount is increased from 5% to 10%. However, as

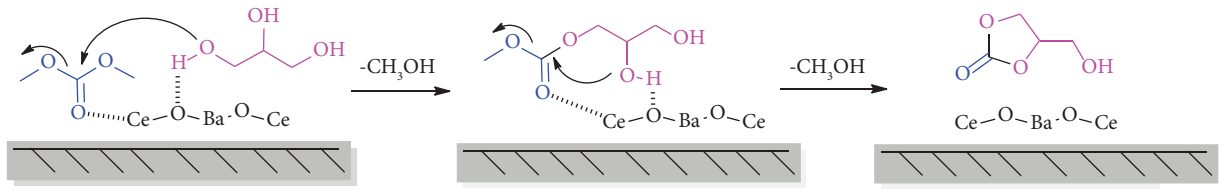

Figure 12: Transesterification of glycerol using a heterogeneous basic catalyst $BaCeO_3$ (adapted from [80]).

the amount of LiCl increased, the yield of GC noticeably decreased because too much LiCl inhibited the activity of the basic sites on the surface of CaO. Moreover, in comparison to commercial CaO, LiCl/CaO improves its surface area from 2.5451 to 3.2822 ($cm^2 \cdot g^{-1}$), and reusability experiment results displayed 80% GC yield after five recycling.

Anionic and basic clay minerals include hydrotalcite, also known as layered double hydroxide (LDH), $(M^{2+}_{(1-x)} M^{3+}_{x}(OH)_2)^{x+}(A_{x/n})^{n-}.yH_2O$. The most common hydrotalcite is $Mg_6Al_2(OH)_{16}CO_{34}H_2O$, traditionally produced via coprecipitation. Since, hydrotalcite shares many of the same chemical and physical characteristics as clay minerals, it is an effective catalyst. They are widely applied in base-catalysed transesterification because their acid-base characteristics can be easily adapted by modifying the composition.

A highly basic heterogeneous catalyst with record activity for GC synthesis was synthesized by Ramesh et al. [52], endorsing Mg-Al LDH and impregnating sodium aluminate ($NaAlO_2$) onto hydrotalcites (Figure 13) with a loading of 5, 10, or 20 wt.% (catalysts denoted as 5 SAHT, 10 SAHT, and 20 SAHT), followed by calcination. Mesopore size on average tends to grow; however, with increasing $NaAlO_2$ loading, specific surface areas decrease along with pore volume. CO_2-TPD experiment was performed for evaluation of catalyst's basicity. Interaction of CO_2 molecules with the surface −OH groups and Mg^{2+}-O^{2-} and Al^{3+}-O^{2-} pairs are the weak basic sites, whereas CO_2 molecules interacting with isolated O^{2-} anions that increased with the increase in $NaAlO_2$ loading are the strong basic sites. Consequently, a sharp rise in total basicity was seen in the reaction. The catalyst showed excellent stability and reusability, easy handling, highly active, and the same glycerol conversion (93%) in the third catalytic cycle which is encouraging from the standpoint of commercial uses.

Hydrocalumite, a layered double hydroxide (LDH) exhibits a highly ordered distribution of anions and water in the interlayer gaps and an organised distribution of Ca-Al ions in the hydroxide layers. In order to transesterify glycerol under mild conditions, Zheng et al. [93] synthesized a series of Ca-Al hydrocalumite with various Ca/Al ratios. The development of a hydrocalumite-like catalyst and a highly ordered of crystallinity in the ratio of Ca/Al = 2–6 were confirmed by the XRD analysis, which detected (002), (004), (010), and (006) planes of hydrocalumite ($Ca_4Al_2O_6Cl_2$, $10H_2O$, JCPDS 00-031- 0245) [100]. 1 : 1 Ca/Al ratio underwent 51% of glycerol conversion, whilst glycerol conversion increased to 75% and GC selectivity remained more than 96% in Ca/Al ratio of 2 : 1. On contrary, conversion, as well as selectivity, gradually dropped on higher Ca/Al ratios (>3 : 1). Inductively coupled plasma-atomic emission spectroscopy (ICP-AES) was used to estimate the Ca-Al hydrocalumite's composition. According to the ICP analysis, which shows that the amount of Ca^{2+} reduced from 12.2 $mmol \cdot g^{-1}$ (for fresh catalyst) to 9.64 $mmol \cdot g^{-1}$ during the recycle experiment, the inactivation of the calcined Ca-Al hydrocalumite was caused by the leaching of Ca in the catalyst (in the six times reused catalyst). Meanwhile, She et al. [101] developed rice-shaped LDH/SBA-15 nanocomposite catalysts (Figure 14) comprising Mg/Al molar ratio of 2 and catalyst loading of 30.46 wt.%, showing promising catalytic activity with a 78% glycerol conversion and 90% selectivity of GC.

By incorporating ZIF-8 with aminopropyl hydroxide imidazole ionic liquid and inserting it in layered Ca-Mg-Al hydrotalcites, Liu et al. [102] developed a novel modified MOF intercalated hydrotalcites known as (APmim)OH/ZIF-8 (refer to Figure 15). In glycerol transesterification with DMC catalysed by (APmim)OH/ZIF-8/LDH in the optimum condition (DMC to glycerol molar ratio 3 : 1, 3 wt.% catalyst loading, 75°C temperature, 80 min) reached glycerol conversion and GC yield of 98.6% and 96.5%, respectively. (APmim)OH/ZIF-8/LDH had a specific surface area of 431.66 $m^2 \cdot g^{-1}$, whereas hydrotalcite CaMgAl-LDH had a specific surface area of around 102.98 $m^2 \cdot g^{-1}$. This high surface area is responsible for high glycerol conversion and yield of GC. However, after being surrounded by microporous ZIF-8, hydrotalcites' average pore size dropped from 17.19 nm to 15.89 nm. The diameter of the ZIF-8 cage was 11.6 Å, whereas the size of the (APmim)OH molecule was 4.15 Å × 4.56 Å × 8.92 Å (Figure 16(a)). After being used five times, the glycerol conversion rate could still reach over 90% owing to (APmim)OH's incorporation into ZIF-8 (Figure 16(b)), which decreased the leaching of active ingredients.

4.2.3. Catalysts from Waste Materials

(1) Plant and Animal Biomass-Derived Catalysts. Biorefineries and the use of renewable sources such as biomass for platform chemicals and catalyst precursor have recently gained popularity as a promising solution for resolving some of these future concerns. In terms of diversity, composition, variability, and abundance, biomass has a great potential to serve as the foundation of biorefinery concepts in future industrial endeavours [103]. Researchers are increasingly focusing on using the biomass waste-derived catalyst for GC generation

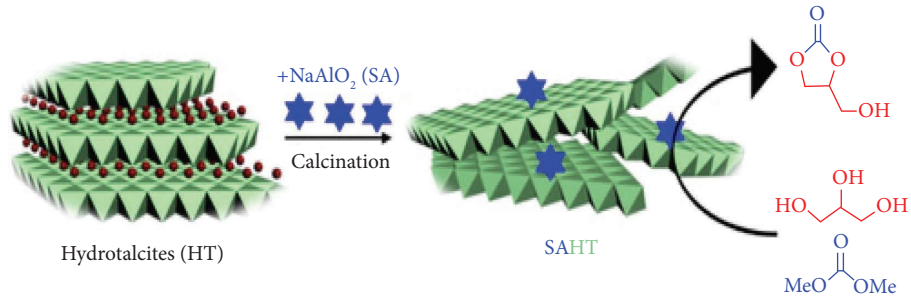

Figure 13: Sodium aluminate hydrotalcite (SAHT) for GC synthesis (reproduced from [52]).

(Table 2, entries 4–13), since this strategy regulates the costs of GC generation while mitigating the disposal issue through transesterification. Changmai et al. [59] researched the efficacy of a solid base catalyst synthesized from *Musa acuminata* peel ash in microwave-assisted glycerol transesterification. The waste-derived catalyst comprised of K_2O (the primary active component) conjuring up 65.9% of the total composition, MgO (2.42%), CaO (7.78%), and SiO_2 (10.86%). Microwave irradiation produced glycerol conversion and GC selectivity of 99% and 99.5%, respectively, under the ideal reaction conditions (2 : 1 molar ratio of DMC/glycerol, 6 wt.% catalyst dosage, 75°C, and 15 min time). Recently, Das et al. [60] utilized *Mangifera indica* peel calcined ash as a catalyst (Figure 17) in glycerol transesterification with DMC under microwave irradiation, which exhibited maximum conversion of 98.1% and improved GC selectivity of 100% under optimal conditions (3 : 1 molar ratio of DMC/glycerol, 6 wt. % catalyst dosage, 80°C, and 50 min reaction time).

As the demand for clean and ecologically friendly sources flourished, researchers discovered more regarding catalysts derived from natural organisms. As the requirement for green and environmentally benign sources increased, researchers gained insight into catalysts derived from natural organisms. Recently, Roschat et al. [63] disclosed a cost-effective, environment-friendly CaO catalyst used in catalytic transesterification. The natural sources for the CaO catalysts include eggshells, cockle shells (CaO_egg, CaO_gol, and CaO_coc), and golden apple snail shells, which were washed, dried, grinded, sieved, and then calcined at 800°C (Table 2, entry 4). Each demonstrated exceptional catalytic activity resulting in successful transesterification, and CaO_coc could provide GC yield of 92.1% within 2 h.

Shikhaliyev et al. [64] were able to create GC, an oxygenated fuel additive by transesterifying excess glycerol with DMC over fishmeal biochar. Fishmeal was calcined at various temperatures ranging from 550 to 750°C. 99.5% GC yield and 100% glycerol conversion were achieved over biochar carbonised at 650°C under the most favourable reaction parameters (DMC to glycerol molar ratio 2 : 1, 85°C, 2 wt.% catalyst loading). Biochar's strong basicity induced decarboxylation reaction that generated glycidol (0.5%). After the fifth reuse, methanol addition without catalyst retained GC yield of 93%. With its low synthesis price, low metal concentration, and easily biodegradable nature, the fishmeal biochar catalyst represents itself as a viable catalyst for commercial purposes.

A crustacean called a crayfish has a lot of calcium in its shell, which is a good raw material for making catalysts for glycerol transesterification. A set of solid base catalysts was developed by Wang et al. [65] using waste crayfish shell powder to synthesize GC. The catalyst produced by calcining waste crayfish shell at 800°C showed significant catalytic activity. Using this catalyst, glycerol conversions of 98.7% and 95.3%,GC yield were attained under optimal reaction conditions (time-90 min, 1 : 6 glycerol to DMC molar ratio, 4 wt.% of catalyst dosage, and 75°C). The rough surface and coarse morphology that arose on the surface of WCSP with a rise in temperature of calcination from 100 to 900°C progressively disappeared with the creation of a relatively smooth surface. The WCSP-800 and WCSP-900 possess total basicity of 20.4 mmol·g^{-1} and 20.5 mmol·g^{-1}, respectively. It was determined that the WCSP-800 was an extremely active catalyst by thoroughly considering the synthetic conditions and the catalysts' preceding characterization results.

GC production driven by oil palm empty fruit bunch ash (EFBA) was explored by Okoye et al. [67]. At temperatures between 300 and 600°C, the catalyst was calcined and the corelationship between catalyst structure, activity, as well as basic endurance was established with the influence of temperature. Results demonstrated that increase in temperature of calcination propagates the phase transition of crystallinity to K_2Mg (SiO_4) from $KAlSiO_4$ by insertion of additional K^+ in the tetrahedral framework of SiO_2 coupled with $Mg^{2+}O^{4-}$. As a result, basic strength of the catalyst was improved, and a substantial number of basic sites were produced, leading to an improvement in the GC yield. At a temperature of 90°C, catalyst dosage of 5 wt.% and an initial DMC to glycerol molar ratio of 3 : 1 and 95.7% GC yield were obtained in 45 minutes of reaction time. Four cycles of reuse resulted in 85.2% yield of GC, showing fairly high stability without significant deactivation. The catalyst is rigid and encompasses heterogeneity to an extensive amount. However, the decline in the catalyst activity was not abrupt.

Preparation of valuable GC was attained by Okoye et al. [58] employing oil palm fuel calcined ash-derived catalyst to prepare valuable GC. Reaction variables were optimized using response surface technique-based Box-Behnken tool, which also improved GC yield and glycerol conversion. GC attained 95% with the desirability of 1 under optimal conditions (80°C, 112 min, 5 : 1 DMC/glycerol molar ratio, 5 wt.% catalyst dosage). At the end of the fifth reuse, glycerol

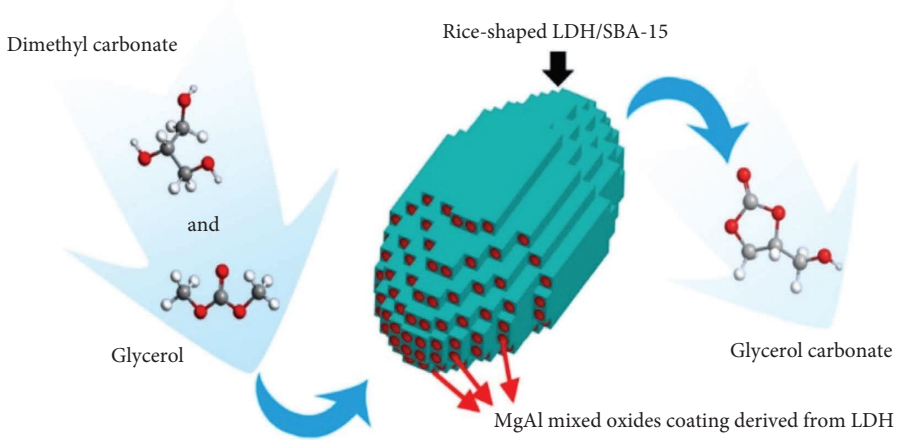

Figure 14: MgAl mixed oxides derived from LDH for GC synthesis (reproduced from [101]).

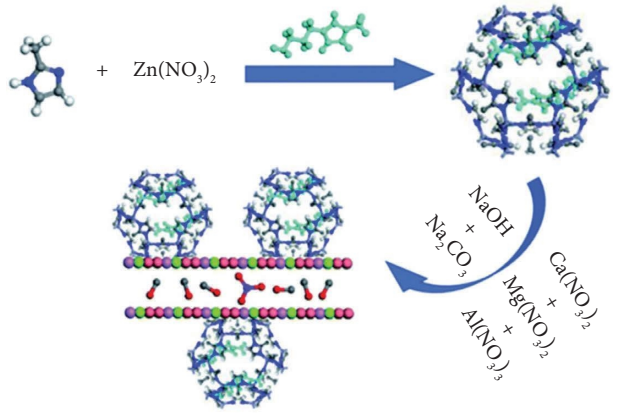

Figure 15: Synthesis diagram of (APmim)OH/ZIF-8/LDH (reproduced from [102]).

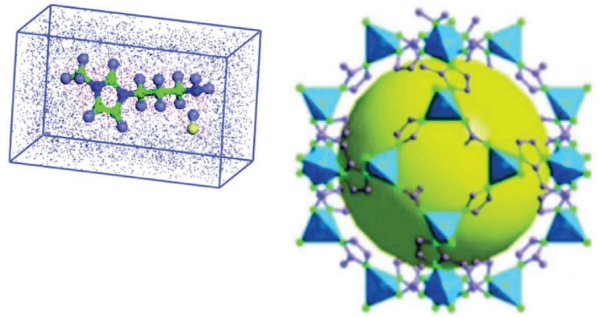

Figure 16: Molecular design of (APmim)OH (a) and ZIF-8 (b) (reproduced from [102]).

conversion and GC yield upheld at around 84.3% and 81.5%, showing that the catalyst possesses a promising prospective for commercialization. According to the EDS findings, the essential mineral elements (K and Mg) necessary for catalysis have been leached, which prompted the decrease in the catalytic activity. Thus, a subsequent decline in the catalyst's overall basic nature (from 12602.98 $mmol \cdot g^{-1}$ to 10882.12 $mmol \cdot g^{-1}$) was observed.

The green synthetic route was explored by Arora et al. [69] utilizing a rice husk-derived catalyst. The catalyst's basic strength varied depending on the metal (cerium) loading (5 wt.% to 20 wt.%) and temperature for calcination (200°C to 500°C). The current research revealed that a catalyst with 10% Ce supported on Na_2SiO_3 surface that had been calcined at 400°C displayed reasonable basic sites with a concentration of 13.89 $mmol \cdot g^{-1}$ and significant catalytic

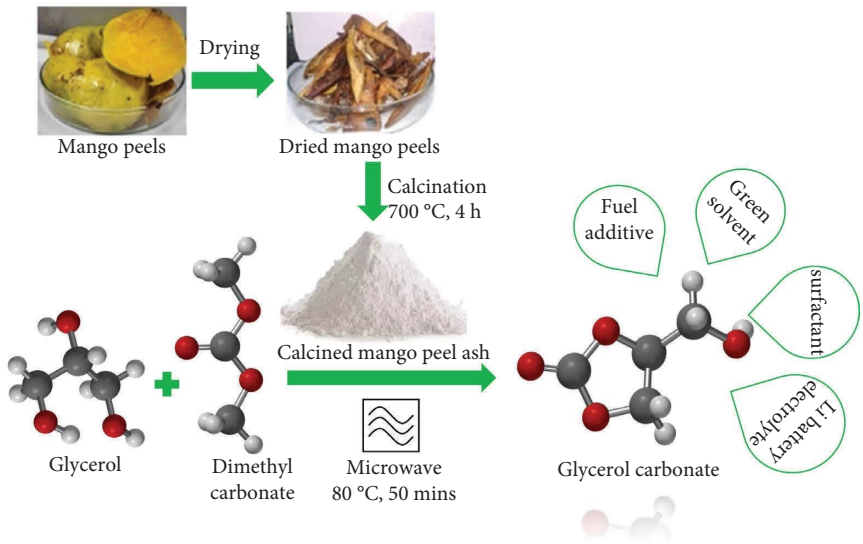

Figure 17: *Mangifera indica* peel calcined ash as catalyst for GC production (reproduced from [60]).

activities. With a dimethyl carbonate: glycerol of 4 : 1 and a 4 wt.% catalyst dosage (based on the weight of glycerol) during a reaction that lasted 150 minutes at 70°C, greater GC yields of 92% and glycerol conversion of 98% were obtained. Better thermal stability up to 600°C was demonstrated by Ce/Na_2SiO_3 (10%, 400°C) without appreciable mass loss. The catalyst stability analysis showed that it might be employed up to four times in a row without losing its catalytic activity. The activation energy was estimated to be 23.80 $KJmol^{-1}$.

(2) Catalysts Derived from General Wastes. General wastes include industrial waste, municipal wastes such as waste red mud from aluminium industry, waste carbide residue, and disposable baby diaper waste (Table 2, entries 1–3). Disposable baby diapers waste-derived catalyst (DBDW) was utilized by Wang et al. [57] for synthesizing GC through transesterification (Figure 18). The most potent solid catalyst was obtained by calcining the superabsorbent polymer in DBDW at various temperatures. The catalyst calcined at 500°C (DBDWS-500) displayed improved catalytic activity even after eight reuses and demonstrated superior catalytic activity (4 : 1 M ratio DMC to glycerol, 75°C, 1 h, 2 wt. % cat.). This maximum catalytic performance was caused by comparatively high concentration of Na_2CO_3-carbonised DBDW matrix.

In order to synthesize GC, Wang et al. [62] introduced Na_2CO_3 onto waste carbide slag (CS) by impregnation-calcination process, thereby developing solid basic catalyst. The catalyst Na_2CO_3-CS-800-15 wt. % was produced by integrating CS into a solution of Na_2CO_3 at a dosage of 15 wt.% of CS and calcining it for three hours at 800°C, demonstrating outstanding catalytic performance. Catalyst concentration of 3 wt% and 5 : 1 DMC to glycerol M ratio yielded 96.0% GC and converted 98.1% glycerol, accomplished in 90 min at 75°C. More crucially, adding Na_2CO_3 can substantially increase the catalyst's capacity for reuse. After five reuses, the 15 wt. % Na_2CO_3-CS-800 may still provide 80.5% GC and convert 83.6% glycerol. Through the generation of a protective $CaCO_3$ shell on the catalyst surface, FTIR and XRD analyses suggested that CO_3^{2-} might be essential in preserving the active catalytic CaO component.

Calcination of waste red mud (RM) derived from aluminium industry was performed at several temperatures from 400°C to 800°C. It was used as catalysts by Das and Mohanty [61] for the effective generation of GC. Before using RM as a catalyst, no chemical pretreatments or insertion of any additional foreign active ingredients into the surface of RM were carried out. By calcining RM at 500°C (RM-500), most catalytic activities (92.02% GC yield) were obtained, according to XRD and FTIR analyses, since it had the highest amount of active $NaAlO_2$ and Ca_2SiO_4 sites. Hematite became the dominant phase at calcination temperatures over 500°C, and the concentrations of $NaAlO_2$ and Ca_2SiO_4 reduced performance of the catalyst. The RM-500 catalyst displayed impressive resistance for transesterifying glycerol in the occurrence of impurities including methanol and water.

4.2.4. Magnetic Catalysts. One of the regular public wastes is diaper waste—about 6% of municipal waste in some nations comprised of diaper waste [104]. More and more emphasis has recently been devoted to manufacture catalysts employing polymer materials [105]. Thus, Wang et al. [106] used polymeric and diaper waste as feedstock to prepare a magnetic heterogeneous catalyst (MHC). To develop a batch of basic MHCs, diaper waste was impregnated in a nickel nitrate solution and then calcined above 400°C. The nomenclature of the as-prepared MHC was DW-Ni-t, where *t* denoted the temperature of the calcination (Table 5, entry 1). Investigations into the structure and catalytic efficiency of the calcined catalysts at various temperatures revealed that the temperature of calcination was a significant factor impacting the catalysts' properties. The catalyst DW-Ni-700

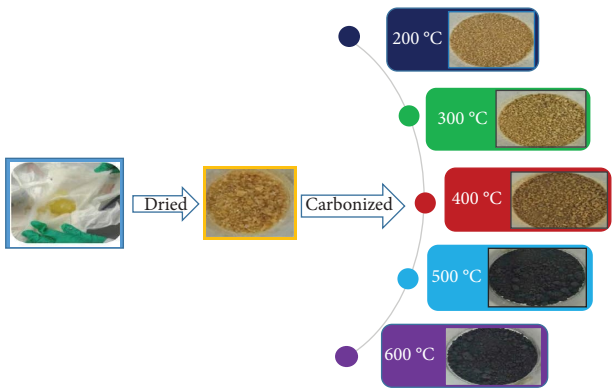

Figure 18: Synthesis of the DBDW-derived catalysts at several temperatures (200°C to 600°C for 30 min) (adapted from [57]).

was found to exhibit the greatest performance. When DW-Ni-700 was used to synthesize GC, its yield increased to 93.2%, and the catalyst separation process was facilitated by DW- Ni-700's magnetic characteristic. Meanwhile, DW-Ni-700 displayed significant reusability (four times) in the reaction and GC yield dropped by less than 4%.

Zhang et al. [107] exploited bifunctional magnetic mesoporous solid base catalyst $CoFe_2O_4$@(CaO-ZnO) for glycerol transesterification. Acidic sites were advantageous for carbonyl-activating DMC to boost GC selectivity, whereas basic sites were helpful for the generation of glyceroxide anion to increase glycerol conversion (Figure 19). The solid base catalyst was easily regained using magnetism. To produce GC through transesterification from glycerol, magnetic mesoporous $CoFe_2O_4$@(CaO-ZnO) demonstrated well catalytic activity. This reaction system produced 96.9% GC yield and 97.7% conversion of glycerol. Vibrating sample magnetometers (VSMs) were used to evaluate the magnetic characteristics of $CoFe_2O_4$ and $CoFe_2O_4$@(CaO-ZnO) at ambient temperature. The saturation magnetization of $CoFe_2O_4$ was 82.7 emu/g, which renders it ferromagnetic. The saturation magnetization of $CoFe_2O_4$@(CaO-ZnO) dropped to 18.2 emu/g due to the encapsulation of CaO and ZnO. However, this value was still sufficient for the separation and recovery of the catalyst.

In another work, for the production of GC, Zhang et al. [108] developed calcium-based magnetic catalysts doped by rare earth metals. Highly efficient magnetic solid catalysts with $NiFe_2O_4$ as magnetic particles have been successfully synthesized. Analysis of the catalysts' basic strength revealed that doping of lanthanum increased basicity reducing particle size to endorse organic reactants close to the catalysts' active sites. With a 99.0% yield of GC, $NiFe_2O_4$@(CaO-La_2O_3) exhibits superior catalytic performance and may be recycled up to six times without noteworthy loss in activity. $NiFe_2O_4$@(CaO-La_2O_3) saturation magnetization decreased from 45.4 to 11.6 emu/g after being covered with calcium oxide and La_2O_3, which could also fulfil separation and recovery requirements.

4.2.5. Nanocatalysts. To produce GC via glycerol transesterification with DMC, Chang et al. [50] produced MgO-loaded ZIF-8 catalysts (MgO@ZIF-8) with different MgO loadings. A wet-impregnation-calcination procedure could deposit MgO nanoparticles onto the surface of ZIF-8 with high atom efficacy upholding the ZIF-8 structure, as revealed by the characterization findings. The microporosity of the ZIF-8 catalyst provides an ideal environment for the very first deposition of Mg precursor and eventual generation of MgO nanoparticles via the nanoconfinement effect. Compared to MgO and ZIF-8, a 50 wt.% MgO@ZIF-8 catalyst was observed to have a higher catalytic activity. Furthermore, the catalyst displayed increased catalytic performance, compared to their mixed counterparts, indicating a synergistic effect between ZIF-8 and MgO. This is clarified by a plausible mechanism (Figure 20) based on the acidic-basic bifunctionality of the surface.

Arora et al. [110] synthesized an active metal CO_3O_4-nanoparticle-containing MCM-41 catalyst produced from rice husk (Table 5, entry 6). The synthesized catalyst's catalytic activity in the transesterification reaction for GC preparation was examined. The synthetic MCM-41 made from rice husk displayed highly ordered p6mm hexagonal symmetry. According to experimental results, 5 wt.% cobalt inserted MCM-41 and activated at 400°C had an increased GC yield of 60.2% because of its ideal basicity. In the optimal conditions (3 : 1 M ratio DMC to glycerol, 90°C, 120 min and 6 wt.% catalyst with respect to concerning glycerol), about 98.7% glycerol conversion and 94.1% GC yield were attained. Using MATLAB's ODE 15s tool, the transesterification process kinetics were also investigated. Calculations revealed that the catalyst's activation energy was 58.2 $KJmol^{-1}$.

The hydrothermal synthetic approach was utilized by Deshmukh et al. [109] to generate several mesoporous polymorphs of MnO_2, and then tested each polymorph's capacity to transesterify glycerol. The most effective, selective, durable, reusable catalyst was MnO_2. For all polymorphs, microwave heating produced maximum conversion with excellent selectivity at 80°C. Conversion of glycerol follows the order as follows: α-$MnO_2 \approx \delta$-$MnO_2 > \beta$-$MnO_2 > \gamma$-MnO_2 > Commercial MnO_2 (least). The order of the trend for the GC selectivity was δ-$MnO_2 > \alpha$-MnO2 > β-$MnO_2 > \gamma$-MnO_2 > Commercial MnO_2. This might be because various polymorphs have varying amphoteric characteristics and surface characteristics. In the microwave-assisted procedure, the GC's selectivity at 80°C was 93%, higher than GC selectivity in the conventional heating method (83%) at 120°C. Using the Scherrer equation, the crystallite sizes for each polymorph were determined to be 1.7, 1.2, 0.6, 1.4, and 1.82 nm for com-MnO_2, respectively.

Glycerol was catalytically transesterified utilizing DMC over MgAl-hydrotalcite (MgAl-HT), CaAl-hydrotalcite (CaAl-HT), and nanostructured CaAl-HT by Devarajan et al. [112]. Ca_4Al-HT was identified to be the one with the highest glycerol conversion (82.4%) and selectivity (95.9%) toward GC. Ca_4Al-HT nanocatalysts (Table 5, entry 8) were synthesized with a different molar concentration of the surfactant (CTAB). Among the catalysts, Ca_4Al-HT 0.4CTAB was found to be the best as it converts 98.7% of glycerol with high selectivity (97.9%) towards GC. Higher desorption temperature and an increase in intensity indicates stronger and higher basicity. Ca_4Al-HT and Mg_4Al-

Table 5: Magnetic mixed metal oxides and nanocatalysts.

Sl. No.	Heterogeneous catalysts	Reaction conditions[a]	Conversion	Selectivity	Yield	Reaction cycles	References
1	DW-Ni-t (t = calcination temperature)	1 : 3, 80, 1, 5	96.6	—	93.2	4	[106]
2	$CoFe_2O_4$@(CaO-ZnO)	1 : 3, 85, 2.5, 0.046 g	97.7	99.2	96.9	5	[107]
3	$NiFe_2O_4$@CaO-La_2O_3	1 : 5, 85, 2, 0.0644 g	99.2	—	99	6	[108]
4	MgO nanoparticles confined in ZIF-8	1 : 4, 75, 2, 0.2 g	—	—	21 mmol/cat	—	[50]
5	MnO_2 nanorods and its different polymorphs	1 : 3, 80, 12 min, 0.027 gcm^{-3}	93	94	—	4	[109]
6	Co_3O_4nanoparticle-incorporated MCM-41 derived from rice husk	1 : 3, 90, 2, 6	98.7	—	94.1	—	[110]
7	CaO-TiO_2 nanocatalyst	1 : 4, 90, 3, 3	99.3	—	93.7	6	[111]
8	Nanostructured CaAl hydrotalcite catalyst (CaAl-HT)	1 : 4, 80, 2, 0.1 g	82.6	97.9		5	[112]

[a]Glycerol: DMC molar ratio, temperature (°C), reaction time (h), and catalyst loading. Note: "—" is not discussed.

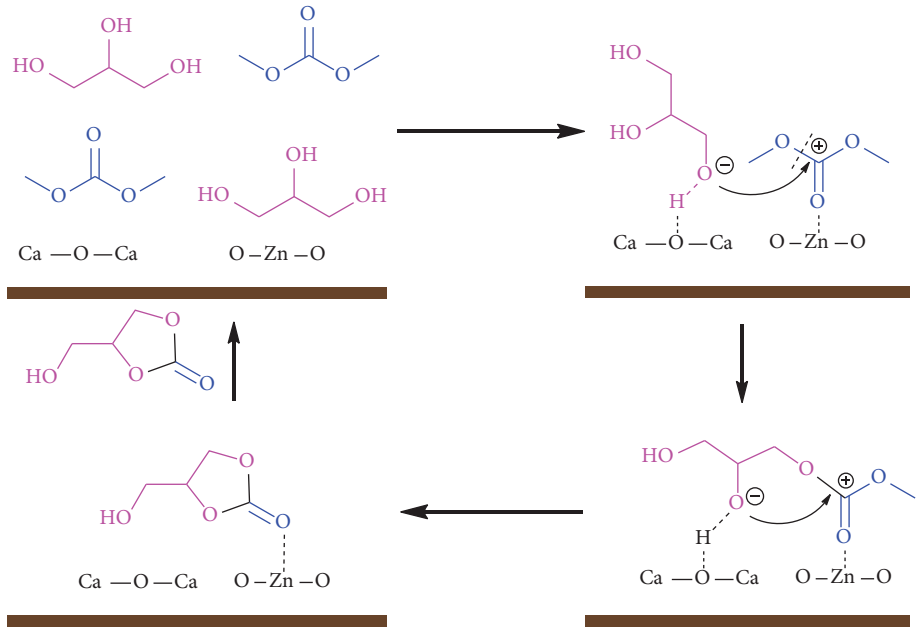

Figure 19: Plausible mechanism of transesterification by acid-base bifunctionalized magnetic solid base catalyst, $CoFe_2O_4$@ (CaO-ZnO) (adapted from [107]).

HT catalysts showed the highest basicity among the corresponding hydrotalcites. The order of basicity as determined by CO_2 desorption is as follows: Ca_4Al-HT > Ca_3Al-HT > Mg_4Al-HT > Ca_2Al-HT > Mg_3Al-HT > Mg_2Al-HT. Recyclability results displayed that the Ca_4Al-HT 0.4CTAB was catalytically active without much loss even after 5 catalytic cycles. The catalyst converted almost 97.8% of glycerol with the selectivity of 97.0% towards GC. This result proves that the Ca_4Al HT 0.4CTAB catalyst is extremely stable.

Focused on a clean catalytic approach, Pradhan and Sharma [111] developed an effective CaO/TiO_2 green nanoparticle synthesized from chicken eggshells with TiO_2 as support for GC production. The 3 : 1 CaO/TiO_2 mixed oxide demonstrated exceptional performance with 99.3% conversion of glycerol and 93.7% GC yield under optimal conditions of reaction parameters (90°C temperature, 180 min time, DMC: glycerol molar ratio 4 : 1, and catalyst loading 3 wt.% w.r.t glycerol). The crystallite size increased from 23 nm to 31 nm after the 3 : 1 Ca/Ti calcination treatment, which may have been caused by the aggregation of CaO at higher calcination temperatures. The catalyst's particle size increased in the following order: $3CaO/TiO_2$ (600°C) < $3CaO/TiO_2$ (700°C) < $3CaO/TiO_2$ (800°C) < $3CaO/TiO_2$ (900°C). The glycerol conversion of the egg shell-derived CaO/TiO_2 mixed oxide was 99.3%, with a yield of 93.7% GC and was stable up to the sixth catalytic cycle under mild reaction conditions.

Utilizing the nonhydrolytic sol-gel (NHSG) methodology, a series of perovskite-based mixed metal oxides (PBMMOs) was generated by Poolwong et al. [113], as a method to produce nanostructured and nonagreeable ternary oxides without calcinating quickly. The most basic PBMMOs ($SrTiO_3$-200, $YNbO_4$-200, and $BaCeO_3$-200) were the most effective catalysts (Figure 21). As a function of the materials basicity, the catalytic behaviour of as-synthesized or calcined PBMMOs displayed a distinct straight-line pattern. Following this, $SrTiO_3$-200 and $YNbO_4$-200, chosen for their catalytic efficacy and low metal toxicity, were used to enhance the atom productivity of this reaction using low (1 : 2 or 1 : 1.5) DMC/glycerol ratios and even equimolar dosages. Using a 1 : 2 DMC/glycerol ratio, $SrTiO_3$-200 catalyst allowed for the glycerol conversion to GC selectively and quantitatively. The catalyst was also capable of being effectively recycled while maintaining a high 95% GC yield during the fifth run. $YNbO_4$-200 (considerably less active than $SrTiO_3$-200) performed satisfactorily, and 80% GC yield was observed. Different magnetic mixed metal oxides and nanocatalysts used for glycerol carbonate production along with their reaction conditions are illustrated in Table 5.

4.3. Enzyme as Biocatalyst. Enzyme catalysis is the process by which glycerol is converted into GC using biological macromolecules made of living cells. Benefits of this catalyst include a rapid rate of conversion, safe reaction conditions, and no harmful residue after use [114]. Recently, enzymes have drawn considerable attention as biocatalysts due to their benign and reusable nature, and their acidic and basic behaviour enzymes or supported enzymes are used as biocatalysts for the generation of GC by transesterification. Table 6 summarizes different enzymes used as biocatalysts in glycerol transesterification with DMC for the GC synthesis.

Candida antarctica lipase B (CALB, Table 6, entry 2), which was immobilised on magnetic organosilica nanoflowers, was utilized by Du et al. [115] for GC production. In addition, it was examined how glycerol/DMC molar ratio, the amount of biocatalyst, temperature, and the time of the reaction affected conversion and selectivity of glycerol and

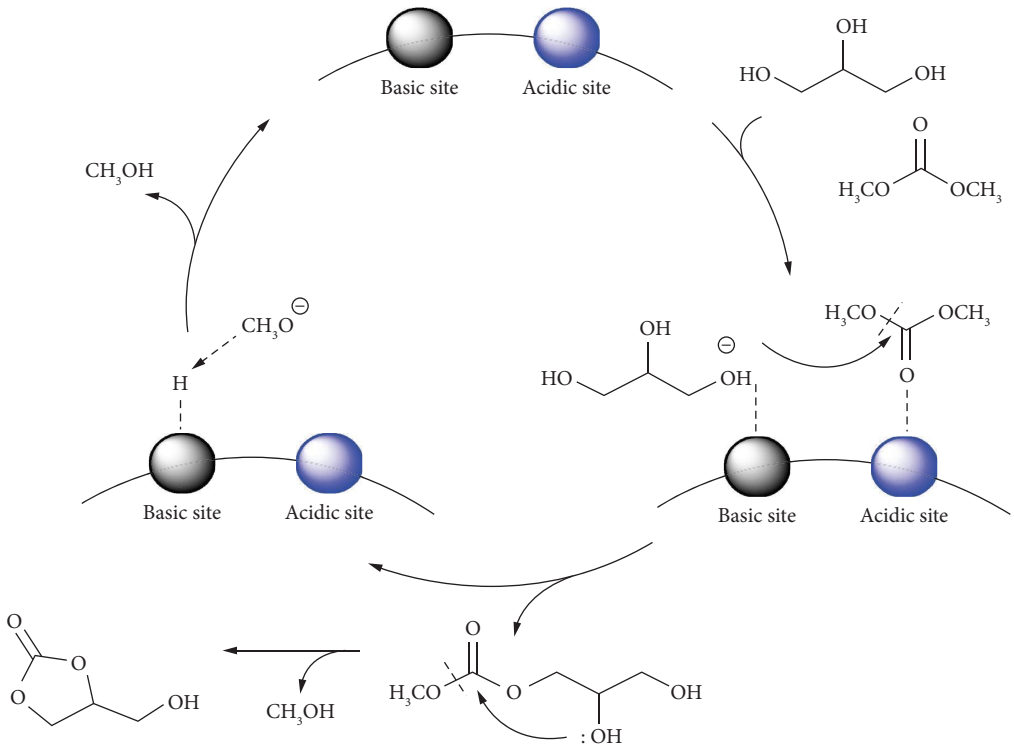

Figure 20: Plausible mechanism of transesterification by acid-base bifunctionalized heterogeneous catalyst (reproduced from [80]).

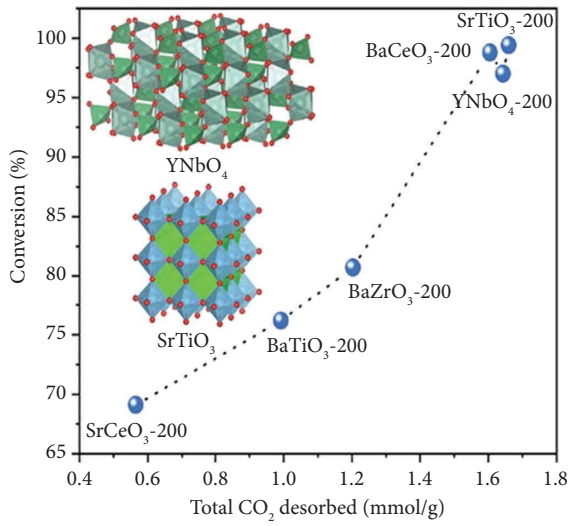

Figure 21: Dependence of turnover frequency amount of glycerol conversion (mol)/(total basic sites ∗ reaction time (h)) of uncalcined and calcined PBMMOs on the number of basic sites for 30 min reaction time (reproduced from [113]).

GC, respectively. Under the conditions of a 20 : 1 M ratio of DMC/glycerol at 50°C and 24 h, the maximum glycerol conversion (94.24%) and yield of GC (88.66%) were perceived. The CALB@nanoflowers (Figure 22) biocatalyst was still able to yield 70.31% GC and achieve a glycerol conversion rate of 79% even after being used seven times.

For the purpose of immobilising enzymes, the colloidosome, an intriguing microcapsule typically made from a Pickering emulsion template, has generated a wave of interest. Using Pickering emulsification, Gao et al. [119] developed a silica-based colloidosome with a magnetic solid core that was employed as an immobilised enzyme system (Figure 23). Hydrophobic-modified Fe_3O_4 nanoparticles were introduced to the oil phase to render the colloidosome magnetic in order to facilitate the separation. The model enzyme used was *Candida antarctica* lipase B (CALB). The adaptability of the LP@colloidosome proved as well in the transesterification-based biosynthesis of GC (Figure 24) that yielded 85.20% of conversion rate at 60°C, employing 6.1 wt.% catalyst.

Table 6: Enzymes as biocatalyst.

Sl. No.	Heterogeneous catalysts	Reaction conditions[a]	Conversion	Selectivity	Yield	Reaction cycles	References
1	Lipase B from *Candida antarctica* immobilised on Accurel MP1000 (CalBAcc)	1 : 3, 60, 48 h, 20	70	90	—	—	[4]
2	Lipase immobilised on magnetic organosilica nanoflowers	1 : 20, 50, 24 h, 5 gL^{-1}	—	94.13	88.53	7	[115]
3	Mixture of lipase B from *C. antarctica* and lipase from porcine pancreas (PPL)	1 : 10, 60, 1.5 h, 20 (w.r.t veg.oil)	—	>99	>99	3	[116]
4	Lipase from *Aspergillus niger*	1 : 10, 60, 4 h, 12	74	80.3	59.3	4	[117]
5	Lipase B from *Candida antarctica* (CaLB) immobilised on Purolite® ECR8214F	1 : 0.3 60, 48 h, 20	46	85	—	—	[118]

[a]Glycerol: DMC molar ratio, temperature (°C), reaction time (h), and catalyst loading. Note: "—" is not discussed.

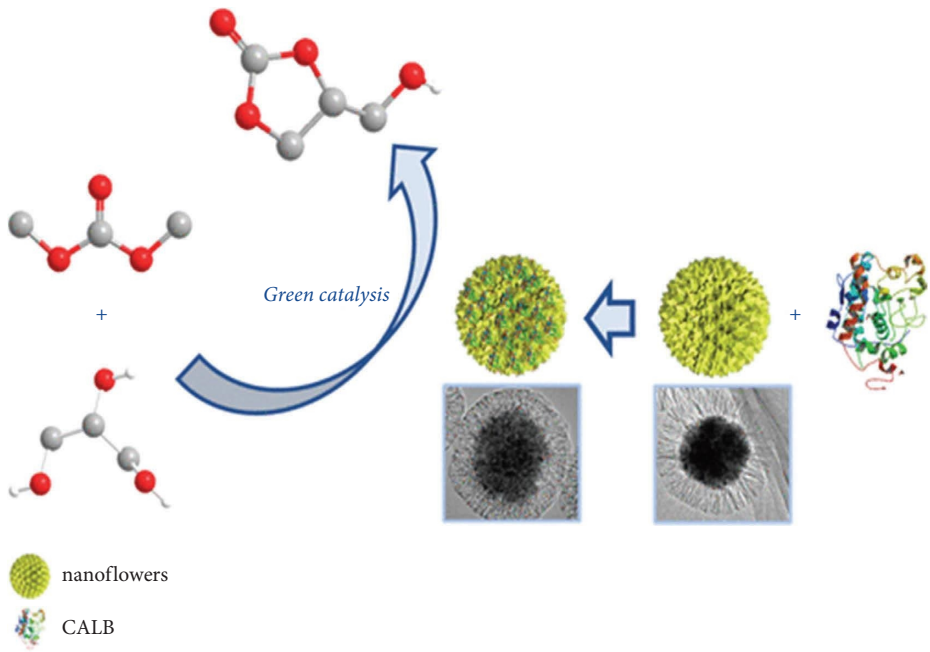

Figure 22: Preparation of CALB@nanoflowers and synthesis of GC catalysed by CALB@nanoflowers (reproduced from [115]).

In order to produce GC by transesterification, Do Nascimento et al. [116] combined lipases from porcine pancreas with *Candida antarctica* immobilised on epoxy resins (Table 6, entry 3). Triacylglycerol and DMC underwent an integrated transesterification reaction in both batch and packed-bed reactors. When commercial Novozym 435 (which has an 88% GC selectivity) was used in place of a homemade immobilised biocatalyst mixture (1 : 1 w/w), the outcome was 100% glycerol conversion and more than 99% GC selectivity. However, due to expensiveness of the enzyme and denaturation over time, the uses of enzymes are restricted for the industrial manufacture of GC.

4.4. Other Catalysts. Beside the usage of categorized heterogeneous catalysts, viz., alkali/alkaline metal oxides, metal supported on metal oxide, plant and animal wastes, and enzymes as biocatalysts for glycerol transesterification to GC, there are also a few more catalysts illustrated in Table 7 which includes ionic liquids, silicates, phosphates, and resins. Application of environmentally benign ionic liquids enhanced the transesterification reaction to produce GC that made it greener and ecofriendlier. Neutral, basic, and acidic ionic liquids were prepared by Miao et al. [120] in two stages. The results confirmed that basic ILs are stronger than inorganic basic catalysts in the transesterification reaction and manifests greater catalytic activity with respect to acidic or neutral ILs. A novel basic IL,1-methyl-3-butylimidazolium imidazolium ([Bmim]Im) was reported which converted 98.4% glycerol and led to GC selectivity of 100% under subsequent optimization reaction conditions (2.5 : 1 DMC to glycerol molar ratio, 70°C, 90 min, and 10 mol % catalyst with respect to glycerol). [Bmim]Im was observed to be stable even after eight times of recycle with 85% glycerol conversion and 90% GC selectivity. The viability is preferably due to strong H-bonding of (IM) anion with the –OH groups of glycerol, ensuing in the synthesis of the corresponding anion and nucleophilic attack on the carbonyl group of dimethyl carbonate, as also proved in one more study by Yi et al. [130].

An efficient strategy was established by Guzmán-Lucero et al. [131] using polyIL catalysts generated from 1-vinylimidazole and comprising the imidazolate anion. The polymeric catalysts demonstrated greater than 90% glycerol conversion when tested using two different concentrations 5 and 10 mol.% of polyILs. One vital benefit is that catalyst could be separated and renewed in two or more reaction cycles without substantial loss in the catalytic activity. The likely chemical pathway to manufacture GC catalysed by polyIL is depicted in Figure 25.

A variety of functionalized quaternary ammonium salt ionic liquids (FQAILs, Table 7, entry 7) were examined by Elhaj et al. [126] in glycerol transesterification to GC utilizing dimethyl carbonate (Figure 26). They noticed that [HPTPA]OH, an ionic liquid with hydroxyl functionalization, had the maximum activity. Under modest conditions of 80°C, 90 min, 3 : 1 DMC/glycerol M ratio, and 0.9 mol % catalyst dosage, they reported 96.2% glycerol conversion and 87.6% GC yield over [HPTPA]OH. They have showed that the [HPTPA]OH catalyst may be recycled minimum three times without significantly losing the catalytic activity.

A set of guanidine-based ILs were investigated by Wang et al. [125] in the glycerol transesterification. With a turnover frequency (TOF) of 1754 h^{-1}, the [TMG][TFE] had an extreme catalytic activity and showed glycerol conversion of 91.8% and 95.5% GC selectivity at reaction temperature 80°C with 0.1 mol % catalyst in half hour. The anion-cation cooperative effect and the modifiable basicity were considered to be the causes of [TMG][TFE] IL's potency. However, ILs

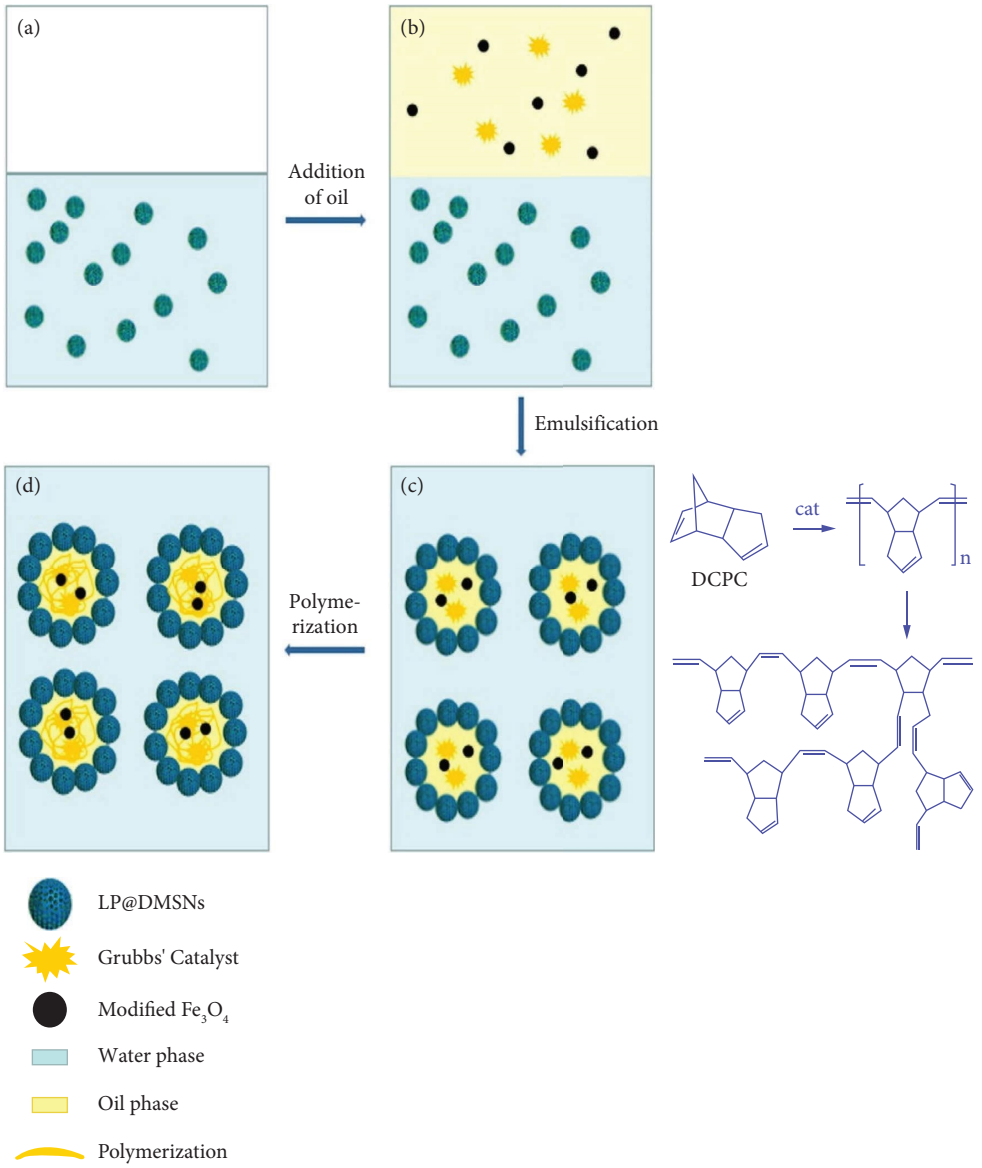

Figure 23: Graphic design of the preparation of LP@colloidosome via the concurrently polymerized inner phase of Pickering emulsion stabilised by LP@DMSNs (reproduced from [119]).

are far more expensive than heterogeneous catalysts, and IL separation is costly, therefore their use is currently confined to the laboratory.

Over the past few decades, organocatalysis has steadily and prominently grown. However, apart from inorganic bases, organic bases such as amines are frequently used as transesterification catalysts, and DABCO (1, 4-diazabicyclo (2.2.2) octane) has confirmed to be a highly effective and homogeneous organic catalyst for the glycerol transesterification [132]. DABCO still has issues with catalyst recovery and reusability due to its homogeneous nature. With the aid of a bifunctional, durable catalyst with a porous organic polymer embedded with DABCO, Lei et al. reported on the organocatalytic glycerol transesterification (Figure 27) [127]. Comparable findings in both activity and selectivity were obtained using this polymer catalyst with outstanding solubilization capacity. Besides, by altering the precursors of polymers, development of catalysts can be easily attained in chemistry.

Comparing several IL catalysts with varied pH, Chen et al. [133] found that the catalyst with an appropriate composition of cation and anion is the way to an effective synthesis. This is because through a hydrogen bonding interaction, the cation and anion of the ionic IL can activate urea and glycerol's –OH group, enabling GC production in selective manner. The catalytic ability of IL is greater than that of conventional metal salt homogeneous catalysts. But these drawbacks substantially restrict their uses because of the challenging preparation, high preparation expense, and limited stability.

In order to overcome the aforementioned difficulties, Simanjuntak et al. [132] observed that ILs with zinc have greater catalytic efficacy. Initially, they synthesized Merrifield peptide resin-supported ionic liquid catalysts

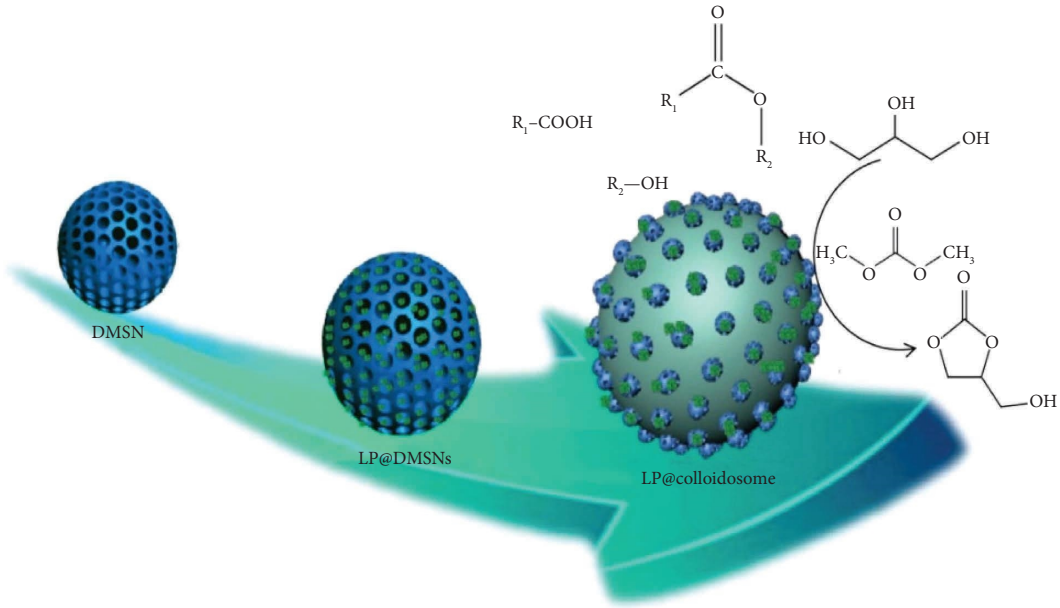

Figure 24: Immobilised enzyme LP@colloidosome for GC production (reproduced from [119]).

(MPR-ILs) which on catalysing the glycerol-urea reaction led to 78.3% conversion of glycerol and 94.4% GC selectivity. Again, later on they discovered polystyrene-based metal comprising imidazolium salts PS-(Im)$_2$ZnBr$_2$ and PS-(Im)$_2$ZnI$_2$ (Figure 28) that not only converted 65.8% and 71.7% glycerol, respectively, but also showed 72.3% and 84.1% selectivity towards GC, respectively. Catalyst of such type is easy to retrieve, isolate, and recycle. In addition, Kim and Park [135] prepared 1-(2-hydroxyethyl) imidazole/$ZnCl_2$ that serves as a bifunctional catalyst seemed to catalyze glycerol-urea reaction at 140°C with 92.7% and 93.4% glycerol conversion rate and GC selectivity, respectively. The catalytic endurance has been greatly enhanced, but the underlying catalysts are difficult and costly to prepare, making them impractical for industrial use. In addition, it is important to highlight that the aforementioned study findings have paved the way for the creation of extremely efficient heterogeneous catalysts.

Okoye et al. [121] valorized glycerol to GC by using anhydrous trisodium phosphate (TSP) catalysed transesterification reaction. Under optimal reaction conditions, TSP showed 99.5% glycerol conversion (Table 7, entry 2) and GC yield as well. The pH of TSP is around 12-13, and the TPD-CO_2 test concluded that there are almost 2.54 mmol·g^{-1} of basic sites of the TSP catalyst surface. With the exception of prominent peaks that were recognised as cubic disodium hydrogen phosphate, the catalyst still showed a maintained tetragonal crystalline phase (Na_2HPO_4) even after the TSP was reused nine times. It is probable that the partial phase change will result in a slight decrease in TSP catalytic performance as polymorph's acidity rises in the order of tribasic < dibasic < monobasic sodium phosphate. TSP catalyst's notable high structural stability is explained by the compact crystalline phase.

Calcined anhydrous sodium silicate (Na_2SiO_3) was utilized as a solid base catalyst by Wang et al. [122] for the generation of GC by transesterification of glycerol. With a glycerol conversion of 97.7%, the calcined Na_2SiO_3 had the best catalytic activity. Glycerol conversion progressively increased with the Na_2SiO_3 catalyst's concentration rising from 1 wt.% to 5 wt.%. In the presence of a 5 wt.% Na_2SiO_3 catalyst, a comparatively high glycerol conversion of 96.7% was attained. This occurred because the Na_2SiO_3 catalyst's active sites were raised as a result of the increase in its amount, which enhanced the conversion of glycerol. In spite of the fact that their bases had equal strengths, Na_2SiO_3 total basicity (10.3 mmol·g^{-1}) was greater than that of CaO (6.8 mmol·g^{-1}). The Na_2SiO_3 catalyst nevertheless produced greater glycerol conversion and GC yield in both temperature constant mode, TCM, (96.7 and 94.3%) and pressure constant mode, PCM, (96.5% and 94.2%) when microwave-assisted transesterification was performed, superior to the CaO catalyst. This solid catalyst could be used up to four times without any noticeable loss of catalytic activity (i.e., 92.5% glycerol conversion).

Later, Devi et al. [124] focused on the progress of a green process for the generation of GC catalysed by the Lewis acidic nature of Ti-SBA-15 catalyst (Table 7, entry 5). For the impregnation of Ti into the silica framework of SBA-15, a sol-gel technique was employed. Ti-SBA-15 (A-E) catalysts with Si/Ti molar ratios ranging from 4 to 32 were developed. When the Si/Ti molar ratio was increased from 4 to 32, it was observed that the GC conversion dropped from 81 to 41%, but there was no noticeable change in the GC's selectivity. According to the BET surface area analysis, the entire pore volume of the catalysts A–E ranged between 0.8 and 1.69 cm^{3}g^{-1}, but SBA–15 had a total pore volume of 1.03 cm^{3}g^{-1}, indicating that the incorporation of Ti into the silica framework in SBA-15 increased the pore volume. According to the results, Ti is present in Ti-SBA-15 catalysts

Table 7: Other heterogeneous catalysts.

Sl. No.	Heterogeneous catalysts	Reaction conditions[a]	Conversion	Selectivity	Yield	Reaction cycles	References
1	Ionic liquid (BMIM-2-CO_2)	1 : 4, 74, 0.5 h, 2	93	99	—	3	[120]
2	Trisodium phosphate (TSP)	1 : 2, 70, 1, 3	99.5	—	99.5	9	[121]
3	Sodium silicate	1 : 4, 95, 15 (temperature constant mode)	96.7	—	94.3	5	[122]
4	Calcined silicates-Na_2SiO_3-200	1 : 4, 75, 2.5, 5	97.8	97.6	95.5	5	[123]
5	Ti-SBA-15	1 : 5, 87.5, 4,	94	—	82	3	[124]
6	Guanidine ILs	1 : 2, 80, 0.5h, 0.1 mol%	91.8	955			[125]
7	FQAILs (HPTPA)OH	1 : 3, 80, 1.5, 0.9 mol%	96.2		87.6	3	[126]
8	DABCO-embedded porous organic polymer	1 : 3,85, 1, 0.4	81.8	80.4	98.3	13	[127]
9	ZrO_2/KOH	1 : 3, 80, 2, 3	99.43	—	—	5	[128]
10	Divinylbenzene Dowex resins	1 : 2, 105, 5, 0.1 g	95	—	45.5	—	[129]

[a]Glycerol: DMC molar ratio, temperature (°C), reaction time (h), and catalyst loading (wt.% w.r.t glycerol mass). Note: "—" is not discussed.

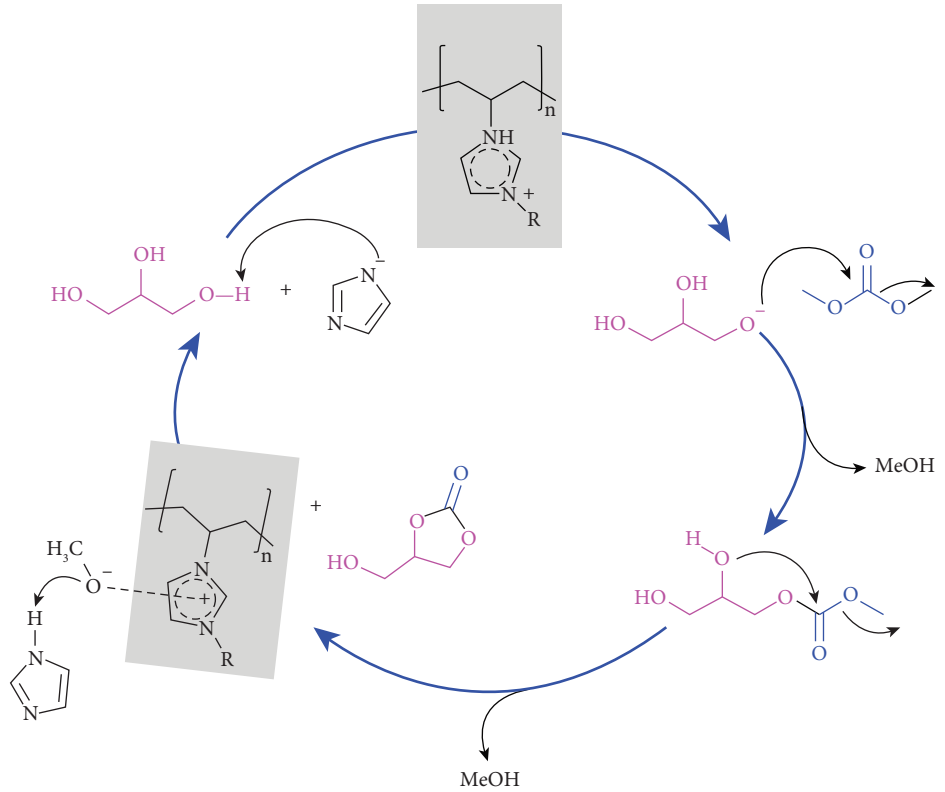

Figure 25: Proposed reaction mechanism to synthesize GC catalysed by polyIL (adapted from [9]).

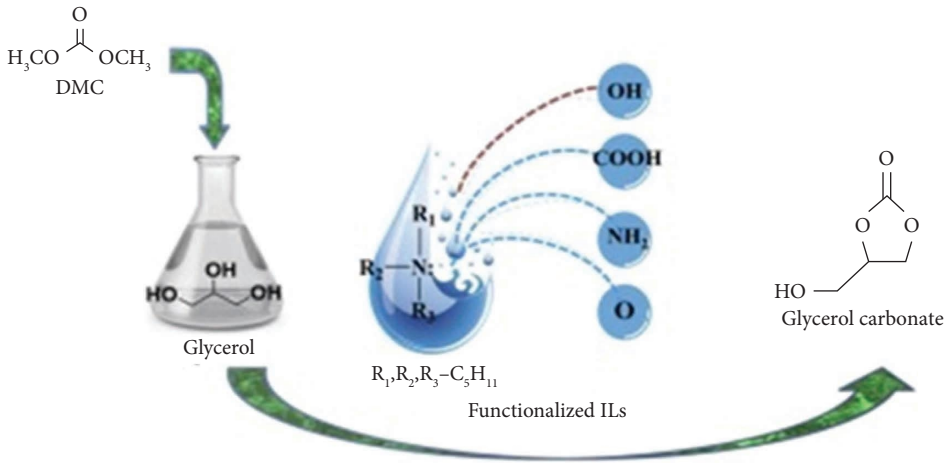

Figure 26: FQAILs for synthesis of GC (reproduced from [126]).

in two phases, which addresses why their catalytic activity is more potent. The extra Ti aggregates as anatase microcrystals outside channels after the initial incorporation of Ti into the silica framework to create a SiO-Ti network. This results in the appearance of various lines linked to crystalline anatase TiO_2, which is supported by the XRD data and further recognised from Raman spectroscopy.

The specifics of how a catalyst's basic strength impacts glycerol conversion and GC selectivity have been adequately reviewed in the following sections.

5. Reaction Parameters Influencing GC Synthesis

The production of GC can be modulated by adjusting the parameters of the transesterification reaction. High glycerol conversion and GC selectivity can be attained by adjusting the process' governing parameters. Several reaction factors, such as catalyst potency, the DMC to glycerol molar ratio, temperature of the reaction, time, rate of stirring, and heating source, affect the rate of adsorption, desorption, and

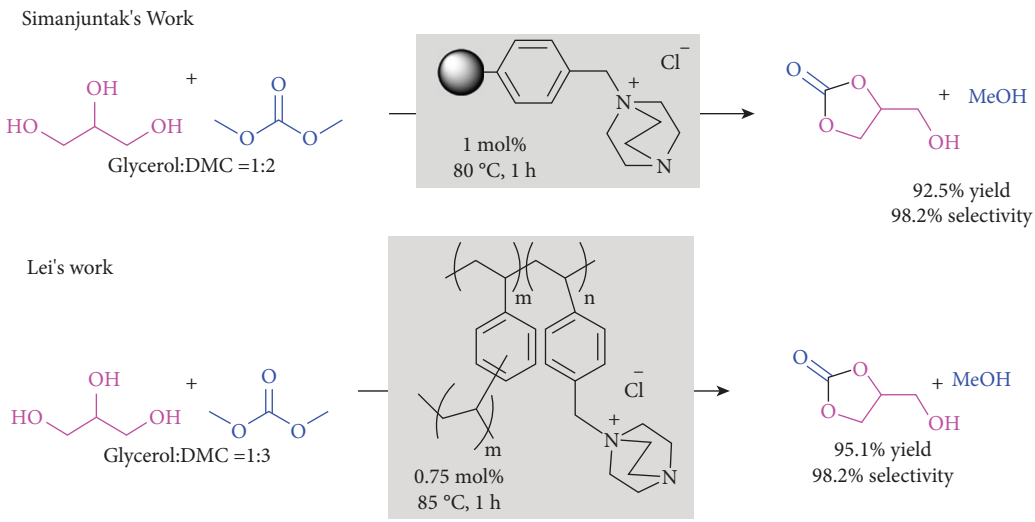

Figure 27: DABCO-modified heterogeneous catalysis in glycerol transesterification (adapted from [80]).

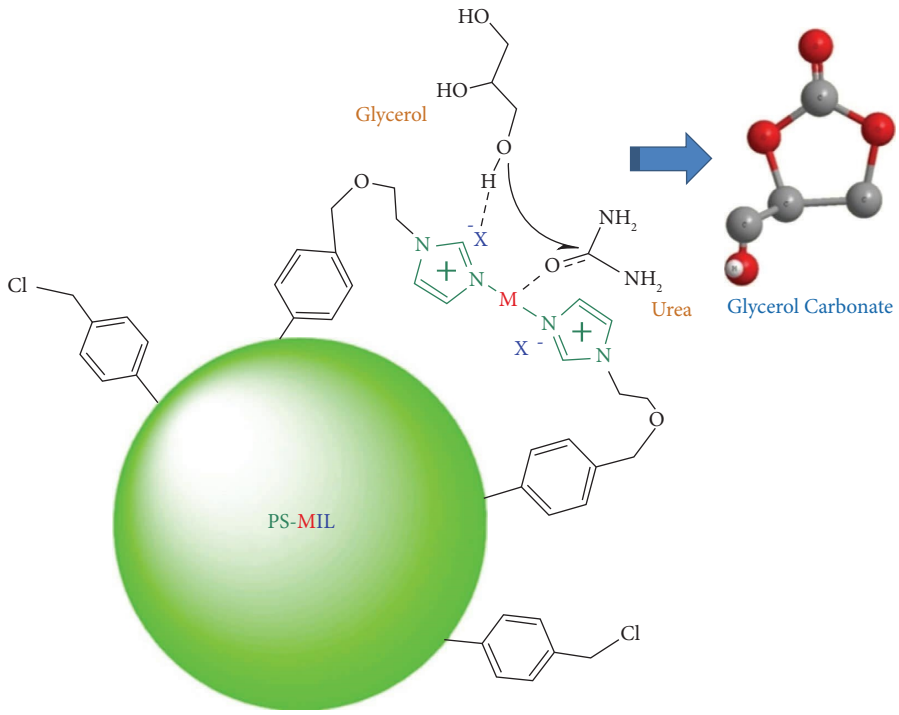

Figure 28: Ionic liquid PS-MIL for GC synthesis via glycerol and urea transesterification (reproduced from[134]).

surface reaction of glycerol transesterification with dimethyl carbonate. The one variable at a time approach was employed by Pradhan and Chandra Sharma [86] to optimize the abovementioned parameters for the maximum glycerol conversion, GC selectivity, and yield of GC. Later, Okoye et al. [58] developed a heterogeneous catalyst from oil palm fuel ash at a reasonable cost and assessed its efficiency in catalysing a transesterification step to produce GC. To increase glycerol conversion and GC yield, reaction parameters were also optimized in this study using response surface methodology (RSM) and the Box-Behnken design. The impact of these reaction parameters on glycerol conversion and GC selectivity is demonstrated in the subsequent sections. Table 8 shows different catalysts used for the GC synthesis.

5.1. Catalyst Loading. The catalyst is vital to the kinetically inert reaction because it provides an alternative route to the reaction that requires less activation energy. A catalyst must contain many active sites that may bind the reactant molecule to one platform in order to execute bond breaking and

Table 8: Different catalysts used and optimized reaction conditions for GC synthesis.

Sl. No.	Catalysts	Reaction conditions[a]	Yield (%)	References
1	Mg/ZnO	1 : 4, 80, 2, 3	90.06	[56]
2	LiCl/CaO	1 : 1, 65, 1, 3	94.19	[92]
3	Hydrotalcites promoted by $NaAlO_2$	1 : 2, 90, 0.5, 3	100	[52]
4	Sr-Al mixed oxide	1 : 2, 70, 1, 3	100	[87]
5	$NaTiO_2$	1 : 2, 90, 1.5, 3	94.5	[97]
6	Calcined *Mangifera indica* peel ash catalyst	1 : 3, 80, 50 min, 6	98.1	[60]
7	Waste carbide slag	1 : 5, 75, 1.5, 3	96	[62]
8	Corncob residue-derived catalyst	1 : 3, 80, 1.5, 3	94.1	[68]
9	Disposable baby diapers waste-derived catalyst	1 : 4, 75, 1, 2	93.6	[57]
10	Porous biochar derived from pyrolysis of fishery waste	1 : 2, 85, 1, 2	99.5	[64]
11	DW-Ni-t (t = calcination temperature)	1 : 3, 80, 1, 5	93.2	[106]
12	Mixture of lipase B from *C. Antarctica* and lipase from porcine pancreas (PPL)	1 : 10, 60, 1.5 h, 20 (w.r.t veg. oil)	>99	[116]

[a]Glycerol: DMC molar ratio, temperature (°C), reaction time (h), and catalyst loading (wt. % w.r.t glycerol mass).

bond building phenomena and produce products, especially in heterogeneous catalysis [136]. Glycerol transesterification has been extensively investigated using heterogeneous catalysts that include primarily alkaline-metal oxides [50, 52, 59] or alkaline mixed metal oxides, surface-modified silicates/hydrotalcites/zeolites [19, 137, 138], mixed metal oxides [54, 139–141], and layered double hydroxides [138]. Alkali metal or alkaline mixed oxide metals have a catalyst loading range of 0.5–5.0 wt.%, whereas bifunctional acid-base and waste-derived catalysts have a range of 3–10 wt.%.

The following explanation is based on several researchers' observations about how basic strength and catalyst loading affect transesterification. The catalytic activity of $Sr_{0.5}$-Al mixed metal oxide in DMC-aided transesterification of glycerol was investigated by Algoufi et al. [87]. The most active phase that produced the maximum quantity of GC was $Sr_3Al_2O_6$. Initially, 3 wt.% catalyst loading increased glycerol conversion to 99.4% with a 94.4% GC yield; however, as catalyst loading increased, the conversion rate decreased and 5% glycidol was produced. Therefore, it can be concluded that due to excess basic strength (beyond the optimal amount), GC decarboxylation forms glycidol, eventually reducing the GC selectivity.

Among all the catalysts discussed in this review and summarized in Table 8, porous biochar derived from pyrolysis of fishery waste (entry 10) as catalyst requires the least catalyst loading of 2 wt.%, producing yield of 99.5%.

5.2. Reaction Time. One of the key elements influencing the transesterification reaction is reaction time. The kinetically labile process takes place faster. As reviewed in Table 4, glycerol and DMC transesterification processes employing heterogeneous catalysts are completed between 15 and 180 minutes. When reactants in a heterogeneous system are miscible, reaction times often increase; alternatively, surface reactions are known to occur more quickly.

By adjusting the reaction period from 60 to 240 minutes, Li et al. [82] investigated the impact of the reaction period during the catalytic synthesis of GC over Li-La_2O_3 catalysts. The reaction did not attain equilibrium during the first hour, as indicated by the 47.9% glycerol conversion and 43.5% GC yield within the first 60 minutes of the reaction. Later, as the reaction progressed, glycerol conversion continued to increase, although GC selectivity remained essentially constant (approximately 92%) from 60 to 180 min of reaction time but decreased to 86.2% at 240 min. This phenomenon results from concurrent side reactions, particularly the etherification of methanol and GC and the breakdown to glycidol. In reality, the considerable decline in GC selectivity during a longer reaction may be driven by the transesterification of glycidol and DMC.

Hydrotalcites promoted by $NaAlO_2$ in just 30 minutes could produce 100% yield of GC, making it the most efficient catalyst among all the catalysts discussed.

5.3. Reaction Temperature. The kinetic hypothesis states that the reaction temperature influences any reaction's rate. An ideal temperature must be chosen for the reaction because it is an independent variable in the reaction coordinate. The Arrhenius equation can be used to correlate the relationship between reaction temperature and reaction rate. The importance of temperature in all chemical processes is explained by the collision theory, which gives a thorough understanding of all chemical reactions. Since the boiling points of hydrophilic glycerol and hydrophobic DMC are 290°C and 90°C, respectively, increasing the temperature above 90°C may cause the evaporation of the DMC, reducing the yield of GC and causing the formation of glycidol through decarboxylation [58, 142, 143]. However, to get excellent yields, the transesterification of glycerol with dimethyl carbonate or diethyl carbonate requires a reaction temperature of 65°C–150°C (Table 4).

The impact of temperatures between 55 and 75°C on the glycerol transesterification process with DMC catalysed by $Sr_{0.5}$-Al mixed oxide was inspected by Algoufi et al. [87]. At 70°C, the process yields a 99.4% GC, but at 55°C, neither the GC yield nor the glycerol conversion was close to 50%. Until 75°C, no further temperature rise resulted in any changes to the GC yield or the conversion of glycerol. In practice, GC yield was significantly reduced when the reaction temperature was raised above 100°C because dehydrogenation and condensation side reactions and glycerol conversion also occurred.

Mixture of lipase B from *C. antarctica* and lipase from porcine pancreas (PPL) biocatalyst achieved greater than 99% GC yield at the lowest temperature requirement of 60°C.

5.4. Effects of Glycerol/DMC Molar Ratio. The glycerol transesterification reaction, which uses DMC as a carbonate source to produce GC, is reversible. Le Chatelier's theory states that equilibrium moves in the direction where stress can be mitigated [136]. Therefore, supplementing the process with an extra amount of DMC could shift the equilibrium toward GC. According to Table 4, DMC: glycerol molar ratio of heterogeneous-catalysed transesterification reaction has consistently been higher than the reaction's stoichiometric ratio. The optimal DMC: glycerol ratio was determined to be between 2 : 1 and 5 : 1, which corresponds to a 15–180 minute reaction period. As the DMC: glycerol molar ratio increased from 1 : 1 to 4 : 1, Pradhan and Chandra Sharma et al. [86] noticed a sharp increase in glycerol conversion and yield of GC (97% and 82%, respectively) by moving the reaction equilibrium to the right. Due to the counterbalancing impact, glycerol concentration functioned as the limiting component; further elevation in glycerol/DMC did not considerably yield notice. According to Wang et al. [57], 4 : 1 DMC: glycerol molar ratio is the suitable value for this component. Further increase in DMC to glycerol ratio did not provide a significant difference.

They also observed that raising the DMC to glycerol molar ratio further did not significantly increase the yield of GC or glycerol conversion. Moreover, among all the catalysts discussed in Table 8, catalyst LiCl/CaO (entry 2) requires the least glycerol: DMC molar ratio leading to a yield of 94.19%.

6. Conclusion and Future Perspectives

The market for glycerol, the principal byproduct of biodiesel synthesis, is saturated due to its surplus production from ever-increasing biodiesel industries. Owing to this, one

highly anticipated downstream glycerol product, GC, has attracted immense attention. This review presents the most current developments' heterogeneous catalysis besides homogeneous catalysis and enzyme catalysis in transesterifying glycerol to GC using dimethyl carbonate. Alkaline-earth metal oxides, doped metal oxides, hydrotalcites, zeolites, ionic liquids, silicates, waste-derived materials, and enzymes are the main focus of heterogeneous catalysts; hence, their applications for the GC synthesis are covered in this critical review. This review also comprises of characterization methods such as SEM, TEM, XRD, BET, XPS, TGA, and NMR for the catalysts and product GC, where significant results have been cited from numerous works. This review's overarching goal is to enlighten readers about the catalytic activity, selectivity, and stability of a variety of heterogeneous catalysts and the factors that lead to their deactivation, so that they may better exploit the vast opportunities they present.

Though this review chiefly discussed the transesterification route and catalytic activity of basic heterogeneous catalysts in GC, there are still many shortcomings in the GC synthesis, and hence it needs special consideration:

(i) More studies are required to produce high-performance catalysts with desirable properties such as improved selectivity and performance, sustainability, exceptional stability, facile separation, and being cheap. Heterogeneous catalysts offer good reusability and simple product separation and can alleviate the issues with homogeneous catalysts and biocatalysts. Moreover, to upgrade the process's cost-effectiveness, generation of heterogeneous catalysts from waste product should be encouraged.

(ii) More raw material optimization, energy consumption reduction, waste emission reduction, reaction step simplification, and cost reduction are all required for successful industrialisation. In an effort to increase demand, the GC market is focusing on downstream sector applications.

(iii) Despite extensive research into catalytic systems' improvement for GC manufacturing, only the transesterification approach using dialkyl carbonates currently appears practical for commercial use. There have been significant advancements made in the direct CO_2 pathway. However, there is still a technology gap that must be filled in order to effectively and inexpensively remove water and shift the equilibrium toward the desired carbonate output.

(iv) The response surface methodology, which finds the optimal reaction conditions by utilizing minimum number of experiments, is the greatest instrument for reaction optimization. This would increase the overall cost-effectiveness of the GC manufacturing process. A suitable reactor configuration is necessary for the large-scale economic synthesis of GC. Unfortunately, there is little information on this topic, and it has to be addressed.

(v) The catalyst reusability is meant to be the foundation of the heterogeneous catalyst. It is the most at risk from deactivation caused by catalyst leaching or self-inactivation.

Data Availability

No data were used in this study.

Conflicts of Interest

The authors declare that they have no conflicts of interest.

References

[1] G. Bagnato, A. Iulianelli, A. Sanna, and A. Basile, "Glycerol production and transformation: a critical review with particular emphasis on glycerol reforming reaction for producing hydrogen in conventional and membrane reactors," *Membranes*, vol. 7, no. 2, p. 17, 2017.

[2] S. Sahani, S. N. Upadhyay, and Y. C. Sharma, "Critical review on production of glycerol carbonate from byproduct glycerol through transesterification," *Industrial and Engineering Chemistry Research*, vol. 60, no. 1, pp. 67–88, 2021.

[3] S. Nomanbhay, M. Y. Ong, K. W. Chew, P. L. Show, M. K. Lam, and W. H. Chen, "Organic carbonate production utilizing crude glycerol derived as by-product of biodiesel production: a review," *Energies*, vol. 13, no. 6, p. 1483, 2020.

[4] R. A. C. Leão, S. P. de Souza, D. O. Nogueira et al., "Consecutive lipase immobilization and glycerol carbonate production under continuous-flow conditions," *Catalysis Science and Technology*, vol. 6, no. 13, pp. 4743–4748, 2016.

[5] P. de Caro, M. Bandres, M. Urrutigoïty, C. Cecutti, and S. Thiebaud-Roux, "Recent progress in synthesis of glycerol carbonate and evaluation of its plasticizing properties," *Frontiers in Chemistry*, vol. 7, pp. 308–313, 2019.

[6] D. Samul, K. Leja, and W. Grajek, "Impurities of crude glycerol and their effect on metabolite production," *Annals of Microbiology*, vol. 64, no. 3, pp. 891–898, 2014.

[7] H. W. Tan, A. R. Abdul Aziz, and M. K. Aroua, "Glycerol production and its applications as a raw material: a review," *Renewable and Sustainable Energy Reviews*, vol. 27, pp. 118–127, 2013.

[8] C. G. Chol, R. Dhabhai, A. K. Dalai, and M. Reaney, "Purification of crude glycerol derived from biodiesel production process: experimental studies and techno-economic analyses," *Fuel Processing Technology*, vol. 178, no. 5, pp. 78–87, 2018.

[9] D. Procopio and M. L. Di Gioia, "An overview of the latest advances in the catalytic synthesis of glycerol carbonate," *Catalysts*, vol. 12, no. 1, p. 50, 2022.

[10] M. J. da Silva, F. de Ávila Rodrigues, and A. A. Júlio, "SnF2-catalyzed glycerol ketalization: a friendly environmentally process to synthesize solketal at room temperature over on solid and reusable Lewis acid," *Chemical Engineering Journal*, vol. 307, pp. 828–835, 2017.

[11] T. Mahreni, T. Marnoto, and M. M. A. Nur, "Production of solketal (2,2-Dimethyl-1,3-dioxolane-4-methanol) from glycerol and acetone by using homogenous acidic catalyst at the boiling temperature (preliminarry study)," *Journal of Physics: Conference Series*, vol. 1295, no. 1, pp. 012004–012009, 2019.

[12] R. Li, H. Song, and J. Chen, "Propylsulfonic acid functionalized sba-15 mesoporous silica as efficient catalysts for the acetalization of glycerol," *Catalysts*, vol. 8, no. 8, p. 297, 2018.

[13] Q. Xie, S. Li, R. Gong et al., "Microwave-assisted catalytic dehydration of glycerol for sustainable production of acrolein over a microwave absorbing catalyst," *Applied Catalysis B: Environmental*, vol. 243, pp. 455–462, 2019.

[14] B. Katryniok, R. Meléndez, V. Bellière-Baca et al., "Catalytic dehydration of glycerol to acrolein in a two-zone fluidized bed reactor," *Frontiers in Chemistry*, vol. 7, p. 127, 2019.

[15] K. A. Lee, H. Ryoo, B. C. Ma, and Y. Kim, "Acrolein production by gas-phase glycerol dehydration using PO 4 /Nb 2 O 5 catalysts," *Journal of Nanoscience and Nanotechnology*, vol. 18, no. 2, pp. 1312–1315, 2018.

[16] J. Shan, Z. Li, S. Zhu et al., "Nanosheet MFI Zeolites for gas phase glycerol dehydration to acrolein," *Catalysts*, vol. 9, no. 2, pp. 121–127, 2019.

[17] B. A. Qureshi, X. Lan, M. T. Arslan, and T. Wang, "Highly active and selective nano h-zsm-5 catalyst with short channels along b-axis for glycerol dehydration to acrolein," *Industrial & Engineering Chemistry Research*, vol. 58, no. 28, pp. 12611–12622, 2019.

[18] T. Ma, J. Ding, X. Liu, G. Chen, and J. Zheng, "Gas-phase dehydration of glycerol to acrolein over different metal phosphate catalysts," *Korean Journal of Chemical Engineering*, vol. 37, no. 6, pp. 955–960, 2020.

[19] P. M. Veiga, A. C. L. Gomes, C. O. Veloso, and C. A. Henriques, "Acid zeolites for glycerol etherification with ethyl alcohol: catalytic activity and catalyst properties," *Applied Catalysis A: General*, vol. 548, pp. 2–15, 2017.

[20] C. Miranda, J. Urresta, H. Cruchade et al., "Exploring the impact of zeolite porous voids in liquid phase reactions: the case of glycerol etherification by tert-butyl alcohol," *Journal of Catalysis*, vol. 365, pp. 249–260, 2018.

[21] F. J. S. Barros, R. Moreno-Tost, J. A. Cecilia et al., "Glycerol oligomers production by etherification using calcined eggshell as catalyst," *Molecular Catalysis*, vol. 433, pp. 282–290, 2017.

[22] L. Aguado-Deblas, R. Estevez, M. Russo, V. La Parola, F. M. Bautista, and M. L. Testa, "Microwave-assisted glycerol etherification over sulfonic acid catalysts," *Materials*, vol. 13, no. 7, pp. 1584–1616, 2020.

[23] S. An, Y. Sun, D. Song, Q. Zhang, Y. Guo, and Q. Shang, "Arenesulfonic acid-functionalized alkyl-bridged organosilica hollow nanospheres for selective esterification of glycerol with lauric acid to glycerol mono- and dilaurate," *Journal of Catalysis*, vol. 342, pp. 40–54, 2016.

[24] N. Binhayeeding, S. Klomklao, and K. Sangkharak, "Utilization of waste glycerol from biodiesel process as a substrate for mono-di-and triacylglycerol production," *Energy Procedia*, vol. 138, pp. 895–900, 2017.

[25] P. Faustino dos Santos, S. R. B. da Silva, F. P. N. R. da Silva, J. D. S. Costa, J. S. Inada, and V. L. P. Pereira, "Green synthesis of glycerol 1,3-bromo- and iodohydrins under solvent-free conditions," *Green Chemistry Letters and Reviews*, vol. 12, no. 4, pp. 389–394, 2019.

[26] M. N. N. Shahirah, J. Gimbun, S. S. Lam, Y. H. Ng, and C. K. Cheng, "Synthesis and characterization of a La–Ni/A-Al2O3 catalyst and its use in pyrolysis of glycerol to syngas," *Renewable Energy*, vol. 132, pp. 1389–1401, 2019.

[27] R. Moreira, A. Moral, F. Bimbela et al., "Syngas production via catalytic oxidative steam reforming of glycerol using a Co/Al coprecipitated catalyst and different bed fillers," *Fuel Processing Technology*, vol. 189, pp. 120–133, 2019.

[28] C. S. Hong, S. Y. Chin, C. Kui Cheng, and G. K. Chua, "Selective oxidation of glycerol to mesoxalic acid by laccase/2,2,6,6-tetramethylpiperidine-N-oxyl system: effect of process conditions and the kinetic modeling," *Chemical Engineering Communications*, vol. 206, no. 12, pp. 1645–1660, 2019.

[29] D. Liu, J. C. Liu, W. Cai et al., "Selective photoelectrochemical oxidation of glycerol to high value-added dihydroxyacetone," *Nature Communications*, vol. 10, no. 1, pp. 1779–1788, 2019.

[30] C. S. Lee, M. K. Aroua, W. A. Wan Daud, P. Cognet, Y. Pérès, and M. A. Ajeel, "Selective electrochemical conversion of glycerol to glycolic acid and lactic acid on a mixed carbon-black activated carbon electrode in a single compartment electrochemical cell," *Frontiers in Chemistry*, vol. 7, pp. 110-111, 2019.

[31] S. Maina, V. Kachrimanidou, D. Ladakis, S. Papanikolaou, A. M. de Castro, and A. Koutinas, "Evaluation of 1,3-propanediol production by two Citrobacter freundii strains using crude glycerol and soybean cake hydrolysate," *Environmental Science and Pollution Research*, vol. 26, no. 35, pp. 35523–35532, 2019.

[32] S. Zhou, S. Lama, M. Sankaranarayanan, and S. Park, "Metabolic engineering of Pseudomonas denitrificans for the 1,3-propanediol production from glycerol," *Bioresource Technology*, vol. 292, Article ID 121933, 2019.

[33] J. Feng, Y. Zhang, W. Xiong, H. Ding, and B. He, "Hydrogenolysis of glycerol to 1,2-propanediol and ethylene glycol over ru-co/zro2 catalysts," *Catalysts*, vol. 6, no. 4, p. 51, 2016.

[34] Z. U. Islam, M. Klein, M. R. Aßkamp, A. S. R. Ødum, and E. Nevoigt, "A modular metabolic engineering approach for the production of 1,2-propanediol from glycerol by *Saccharomyces cerevisiae*," *Metabolic Engineering*, vol. 44, pp. 223–235, 2017.

[35] F. Cai, F. Jin, J. Hao, and G. Xiao, "Selective hydrogenolysis of glycerol to 1,2-propanediol on Nb-modified Pd–Zr–Al catalysts," *Catalysis Communications*, vol. 131, no. 8, Article ID 105801, 2019.

[36] T. S. de Andrade, M. M. V. M. Souza, and R. L. Manfro, "Hydrogenolysis of glycerol to 1,2-propanediol without external H2 addition in alkaline medium using Ni-Cu catalysts supported on Y zeolite," *Renewable Energy*, vol. 160, pp. 919–930, 2020.

[37] É. V. de Oliveira, H. Brasil, G. P. Valença, and E. Jordão, "Tuning the synthesis pH and composition of Cu hydrotalcites for hydrogenolysis of glycerol," *Catalysis Communications*, vol. 136, Article ID 105925, 2020.

[38] Y. Liu, X. Guo, G. L. Rempel, and F. T. T. Ng, "The promoting effect of Ni on glycerol hydrogenolysis to 1,2-propanediol with in situ hydrogen from methanol steam reforming using a Cu/Zno/Al2O3 catalyst," *Catalysts*, vol. 9, no. 5, p. 412, 2019.

[39] N. Zanda, A. Sobolewska, E. Alza, A. W. Kleij, and M. A. Pericàs, "Organocatalytic and halide-free synthesis of glycerol carbonate under continuous flow," *ACS Sustainable Chemistry and Engineering*, vol. 9, no. 12, pp. 4391–4397, 2021.

[40] N. Yadav, F. Seidi, S. Del Gobbo, V. D'Elia, and D. Crespy, "Versatile functionalization of polymer nanoparticles with carbonate groups via hydroxyurethane linkages," *Polymer Chemistry*, vol. 10, no. 26, pp. 3571–3584, 2019.

[41] N. Bragato and G. Fiorani, "Cyclic organic carbonates from furanics: opportunities and challenges," *Current Opinion in Green and Sustainable Chemistry*, vol. 30, Article ID 100479, 2021.

[42] S. Christy, A. Noschese, M. Lomelí-Rodriguez, N. Greeves, and J. A. Lopez-Sanchez, "Recent progress in the synthesis and applications of glycerol carbonate," *Current Opinion in Green and Sustainable Chemistry*, vol. 14, pp. 99–107, 2018.

[43] G. Fiorani, A. Perosa, and M. Selva, "Dimethyl carbonate: a versatile reagent for a sustainable valorization of renewables," *Green Chemistry*, vol. 20, no. 2, pp. 288–322, 2018.

[44] J. Ochoa-Gómez, O. Gómez-Jiménez-Aberasturi, C. Ramírez-López, and M. Belsué, "A brief review on industrial alternatives for the manufacturing of glycerol carbonate, a Green Chemical," *Organic Process Research and Development*, vol. 16, no. 3, pp. 389–399, 2012.

[45] M. J. Climent, A. Corma, P. De Frutos et al., "Chemicals from biomass: synthesis of glycerol carbonate by transesterification and carbonylation with urea with hydrotalcite catalysts. The role of acid-base pairs," *Journal of Catalysis*, vol. 269, no. 1, pp. 140–149, 2010.

[46] J. Li and T. Wang, "Coupling reaction and azeotropic distillation for the synthesis of glycerol carbonate from glycerol and dimethyl carbonate," *Chemical Engineering and Processing: Process Intensification*, vol. 49, no. 5, pp. 530–535, 2010.

[47] W. K. Teng, R. Yusoff, M. K. Aroua, and G. C. Ngoh, "Process optimization and kinetics of microwave assisted transesterification of crude glycerol for the production of glycerol carbonate," *Sustainable Energy Fuels*, vol. 5, no. 1, pp. 274–282, 2021.

[48] W. K. Teng, G. C. Ngoh, R. Yusoff, and M. K. Aroua, "A review on the performance of glycerol carbonate production via catalytic transesterification: effects of influencing parameters," *Energy Conversion and Management*, vol. 88, pp. 484–497, 2014.

[49] M. Aresta, A. Dibenedetto, F. Nocito, and C. Ferragina, "Valorization of bio-glycerol: new catalytic materials for the synthesis of glycerol carbonate via glycerolysis of urea," *Journal of Catalysis*, vol. 268, no. 1, pp. 106–114, 2009.

[50] C. W. Chang, Z. J. Gong, N. C. Huang, C. Y. Wang, and W. Y. Yu, "MgO nanoparticles confined in ZIF-8 as acid-base bifunctional catalysts for enhanced glycerol carbonate production from transesterification of glycerol and dimethyl carbonate," *Catalysis Today*, vol. 351, pp. 21–29, 2020.

[51] M. Tudorache, A. Negoi, and V. I. Parvulescu, "Enhancement of the valorization of renewable glycerol: the effects of the surfactant-enzyme interaction on the biocatalytic synthesis of glycerol carbonate," *Catalysis Today*, vol. 279, pp. 71–76, 2017.

[52] S. Ramesh, F. Devred, L. van den Biggelaar, and D. P. Debecker, "Hydrotalcites promoted by NaAlO2 as strongly basic catalysts with record activity in glycerol carbonate synthesis," *ChemCatChem*, vol. 10, no. 6, pp. 1398–1405, 2018.

[53] G. Parameswaram, P. S. N. Rao, A. Srivani, G. N. Rao, and N. Lingaiah, "Magnesia-ceria mixed oxide catalysts for the selective transesterification of glycerol to glycerol carbonate," *Molecular Catalysis*, vol. 451, pp. 135–142, 2018.

[54] Y. Wu, X. Song, J. Zhang et al., "Synthesis of glycerol carbonate from glycerol and diethyl carbonate over CeO2-CdO catalyst: the role of Ce4+ doped into CdO lattice," *Journal of the Taiwan Institute of Chemical Engineers*, vol. 87, pp. 131–139, 2018.

[55] S. Jaiswal, G. Pradhan, and Y. C. Sharma, "Green and facile synthesis of glycerol carbonate from bio-glycerol assisted by lithium titanate: a robust and selective heterogeneous catalyst," *Journal of the Taiwan Institute of Chemical Engineers*, vol. 128, pp. 388–399, 2021.

[56] G. Pradhan and Y. C. Sharma, "Green synthesis of glycerol carbonate by transesterification of bio glycerol with dimethyl carbonate over Mg / ZnO: A highly efficient heterogeneous catalyst," *Fuel*, vol. 284, Article ID 118966, 2021.

[57] S. Wang, J. Wang, P. Sun et al., "Disposable baby diapers waste derived catalyst for synthesizing glycerol carbonate by the transesterification of glycerol with dimethyl carbonate," *Journal of Cleaner Production*, vol. 211, pp. 330–341, 2019.

[58] P. U. Okoye, S. Wang, W. A. Khanday, S. Li, T. Tang, and L. Zhang, "Box-Behnken optimization of glycerol transesterification reaction to glycerol carbonate over calcined oil palm fuel ash derived catalyst," *Renewable Energy*, vol. 146, pp. 2676–2687, 2020.

[59] B. Changmai, I. B. Laskar, and L. Rokhum, "Microwave-assisted synthesis of glycerol carbonate by the transesterification of glycerol with dimethyl carbonate using Musa acuminata peel ash catalyst," *Journal of the Taiwan Institute of Chemical Engineers*, vol. 102, pp. 276–282, 2019.

[60] A. Das, D. Shi, G. Halder, S. Lalthazuala Rokhum, and S. Lalthazuala, "Microwave-assisted synthesis of glycerol carbonate by transesterification of glycerol using Mangifera indica peel calcined ash as catalyst," *Fuel*, vol. 330, Article ID 125511, 2022.

[61] B. Das and K. Mohanty, "A green and facile production of catalysts from waste red mud for the one-pot synthesis of glycerol carbonate from glycerol," *Journal of Environmental Chemical Engineering*, vol. 7, no. 1, Article ID 102888, 2019.

[62] J. Wang, Z. Wang, H. Liu, S. Wang, and Y. Sun, "Synthesis of glycerol carbonate from glycerol and dimethyl carbonate catalyzed by solid base catalyst derived from waste carbide slag," *International Journal of Polymer Science*, vol. 2021, Article ID 9300442, 14 pages, 2021.

[63] W. Roschat, S. Phewphong, T. Kaewpuang, and V. Promarak, "Synthesis of glycerol carbonate from transesterification of glycerol with dimethyl carbonate catalyzed by CaO from natural sources as green and economical catalyst," *Materials Today: Proceedings*, vol. 5, no. 6, pp. 13909–13915, 2018.

[64] K. Shikhaliyev, P. U. Okoye, and B. H. Hameed, "Transesterification of biodiesel byproduct glycerol and dimethyl carbonate over porous biochar derived from pyrolysis of fishery waste," *Energy Conversion and Management*, vol. 165, pp. 794–800, 2018.

[65] J. Wang, H. Liu, Z. Chen, Y. Sun, and S. Wang, "Using waste crayfish shell derived catalyst to synthesize glycerol carbonate by transesterification reaction between glycerol and dimethyl carbonate," *Reaction Kinetics, Mechanisms and Catalysis*, vol. 133, no. 1, pp. 191–208, 2021.

[66] Y. T. Algoufi and B. H. Hameed, "Synthesis of glycerol carbonate by transesterification of glycerol with dimethyl carbonate over K-zeolite derived from coal fly ash," *Fuel Processing Technology*, vol. 126, pp. 5–11, 2014.

[67] P. U. Okoye, S. Wang, L. Xu, S. Li, J. Wang, and L. Zhang, "Promotional effect of calcination temperature on structural evolution, basicity, and activity of oil palm empty fruit bunch derived catalyst for glycerol carbonate synthesis," *Energy Conversion and Management*, vol. 179, pp. 192–200, 2019.

[68] S. Wang, J. Wang, P. U. Okoye et al., "Application of corncob residue-derived catalyst in the transesterification of glycerol

with dimethyl carbonate to synthesize glycerol carbonate," *Bioresources*, vol. 15, no. 1, pp. 142–158, 2019.

[69] S. Arora, V. Gosu, U. K. Arun Kumar, and V. Subbaramaiah, "A facile approach to develop rice husk derived green catalyst for one-pot synthesis of glycerol carbonate from glycerol," *International Journal of Chemical Reactor Engineering*, vol. 18, no. 3, pp. 1–16, 2020.

[70] M. A. Borysiewicz, "ZnO as a functional material, A review," *Crystals*, vol. 9, no. 10, p. 505, 2019.

[71] J. Poolwong, V. Aomchad, S. Del Gobbo, A. W. Kleij, and V. D'Elia, "Simple halogen-free, Biobased organic salts convert glycidol to glycerol carbonate under atmospheric CO 2 pressure," *ChemSusChem*, vol. 15, no. 17, Article ID 202200765, 2022.

[72] J. Esteban, E. Domínguez, M. Ladero, and F. Garcia-Ochoa, "Kinetics of the production of glycerol carbonate by transesterification of glycerol with dimethyl and ethylene carbonate using potassium methoxide, a highly active catalyst," *Fuel Processing Technology*, vol. 138, pp. 243–251, 2015.

[73] B. Hervert, P. D. McCarthy, and H. Palencia, "Room temperature synthesis of glycerol carbonate catalyzed by N-heterocyclic carbenes," *Tetrahedron Letters*, vol. 55, no. 1, pp. 133–136, 2014.

[74] G. Rokicki, P. Rakoczy, P. Parzuchowski, and M. Sobiecki, "Hyperbranched aliphatic polyethers obtained from environmentally benign monomer: glycerol carbonate," *Green Chemistry*, vol. 7, no. 7, pp. 529–539, 2005.

[75] J. R. Ochoa-Gómez, O. Gómez-Jiménez-Aberasturi, B. Maestro-Madurga et al., "Synthesis of glycerol carbonate from glycerol and dimethyl carbonate by transesterification: catalyst screening and reaction optimization," *Applied Catalysis A: General*, vol. 366, no. 2, pp. 315–324, 2009.

[76] Z. Herseczki, T. Varga, and G. Marton, "Synthesis of glycerol carbonate from glycerol, a by-product of biodiesel production," *International Journal of Chemical Reactor Engineering*, vol. 7, no. 1, 2009.

[77] J. R. Ochoa-Gómez, O. Gómez-Jiménez-Aberasturi, C. Ramírez-López, and B. Maestro-Madurga, "Synthesis of glycerol 1,2-carbonate by transesterification of glycerol with dimethyl carbonate using triethylamine as a facile separable homogeneous catalyst," *Green Chemistry*, vol. 14, no. 12, pp. 3368–3376, 2012.

[78] Z. Wang, "Green chemistry: recent advances in developing catalytic processes in environmentally-benign solvent systems," *Frontiers in Chemistry*, vol. 28, no. 7, pp. 1–43, 2008.

[79] J. Esteban, E. Fuente, A. Blanco, M. Ladero, and F. Garcia-Ochoa, "Phenomenological kinetic model of the synthesis of glycerol carbonate assisted by focused beam reflectance measurements," *Chemical Engineering Journal*, vol. 260, pp. 434–443, 2015.

[80] Y. Ji, "Recent development of heterogeneous catalysis in the transesterification of glycerol to glycerol carbonate," *Catalysts*, vol. 9, no. 7, p. 581, 2019.

[81] X. Song, Y. Wu, F. Cai, D. Pan, and G. Xiao, "High-efficiency and low-cost Li/ZnO catalysts for synthesis of glycerol carbonate from glycerol transesterification: the role of Li and ZnO interaction," *Applied Catalysis A: General*, vol. 532, pp. 77–85, 2017.

[82] Y. Li, J. Liu, and D. He, "Catalytic synthesis of glycerol carbonate from biomass-based glycerol and dimethyl carbonate over Li-La2O3 catalysts," *Applied Catalysis A: General*, vol. 564, pp. 234–242, 2018.

[83] K. Hu, H. Wang, Y. Liu, and C. Yang, "KNO3/CaO as cost-effective heterogeneous catalyst for the synthesis of glycerol carbonate from glycerol and dimethyl carbonate," *Journal of Industrial and Engineering Chemistry*, vol. 28, pp. 334–343, 2015.

[84] Z. Liu, J. Wang, M. Kang et al., "Structure-activity correlations of $LiNO_3/Mg_4AlO_{5.5}$ catalysts for glycerol carbonate synthesis from glycerol and dimethyl carbonate," *Journal of Industrial and Engineering Chemistry*, vol. 21, pp. 394–399, 2015.

[85] Y. T. Algoufi, G. Kabir, and B. H. Hameed, "Synthesis of glycerol carbonate from biodiesel by-product glycerol over calcined dolomite," *Journal of the Taiwan Institute of Chemical Engineers*, vol. 70, pp. 179–187, 2017.

[86] G. Pradhan and Y. Chandra Sharma, "Studies on green synthesis of glycerol carbonate from waste cooking oil derived glycerol over an economically viable NiMgOx heterogeneous solid base catalyst," *Journal of Cleaner Production*, vol. 264, Article ID 121258, 2020.

[87] Y. T. Algoufi, U. G. Akpan, G. Kabir, M. Asif, and B. H. Hameed, "Upgrading of glycerol from biodiesel synthesis with dimethyl carbonate on reusable Sr–Al mixed oxide catalysts," *Energy Conversion and Management*, vol. 138, pp. 183–189, 2017.

[88] M. Marimuthu, P. Marimuthu, A. K. Sk, S. Palanivelu, and V. Rajagopalan, "Tuning the basicity of Cu-based mixed oxide catalysts towards the efficient conversion of glycerol to glycerol carbonate," *Molecular Catalysis*, vol. 460, pp. 53–62, 2018.

[89] P. Kumar, P. With, V. C. Srivastava, R. Gläser, and I. M. Mishra, "Glycerol carbonate synthesis by hierarchically structured catalysts: catalytic activity and characterization," *Industrial & Engineering Chemistry Research*, vol. 54, no. 50, pp. 12543–12552, 2015.

[90] P. P. Pattanaik, P. M. Kumar, N. Raju, and N. Lingaiah, "Continuous synthesis of glycerol carbonate by transesterification of glycerol with dimethyl carbonate over Fe–La mixed oxide catalysts," *Catalysis Letters*, vol. 151, no. 5, pp. 1433–1443, 2021.

[91] G. Liu, J. Yang, and X. Xu, "Synthesis of hydrotalcite-type mixed oxide catalysts from waste steel slag for transesterification of glycerol and dimethyl carbonate," *Scientific Reports*, vol. 10, no. 1, pp. 10273–10314, 2020.

[92] Y. Tang, Y. Y. Xue, Z. Li, T. Yan, R. Zhou, and Z. Zhang, "Heterogeneous synthesis of glycerol carbonate from glycerol and dimethyl carbonate catalyzed by LiCl/CaO," *Journal of Saudi Chemical Society*, vol. 23, no. 4, pp. 494–502, 2019.

[93] L. Zheng, S. Xia, X. Lu, and Z. Hou, "Transesterification of glycerol with dimethyl carbonate over calcined Ca-Al hydrocalumite," *Chinese Journal of Catalysis*, vol. 36, no. 10, pp. 1759–1765, 2015.

[94] J. Granados-Reyes, P. Salagre, and Y. Cesteros, "Effect of the preparation conditions on the catalytic activity of calcined Ca/Al-layered double hydroxides for the synthesis of glycerol carbonate," *Applied Catalysis A: General*, vol. 536, pp. 9–17, 2017.

[95] J. Keogh, G. Deshmukh, and H. Manyar, "Green synthesis of glycerol carbonate via transesterification of glycerol using mechanochemically prepared sodium aluminate catalysts," *Fuel*, vol. 310, Article ID 122484, 2022.

[96] A. Chotchuang, P. Kunsuk, A. Phanpitakkul, S. Chanklang, M. Chareonpanich, and A. Seubsai, "Production of glycerol carbonate from glycerol over modified sodium-aluminate-doped calcium oxide catalysts," *Catalysis Today*, vol. 388, pp. 351–359, 2022.

[97] S. Jaiswal, S. Sahani, and Y. C. Shar, "Enviro-benign synthesis of glycerol carbonate utilizing bio-waste glycerol over Na-Ti based heterogeneous catalyst: kinetics and E- metrics studies," *Journal of Environmental Chemical Engineering*, vol. 10, no. 3, Article ID 107485, 2022.

[98] Z. Liu, B. Li, F. Qiao et al., "Catalytic performance of Li/Mg composites for the synthesis of glycerol carbonate from glycerol and dimethyl carbonate," *ACS Omega*, vol. 7, no. 6, pp. 5032–5038, 2022.

[99] A. F. Lee and K. Wilson, "Recent developments in heterogeneous catalysis for the sustainable production of biodiesel," *Catalysis Today*, vol. 242, pp. 3–18, 2015.

[100] S. Kim, C. M. Park, M. Jang et al., "Aqueous removal of inorganic and organic contaminants by graphene-based nanoadsorbents: A review," *Chemosphere*, vol. 212, pp. 1104–1124, 2018.

[101] Q. M. She, W. J. Huang, A. Talebian-kiakalaieh, H. Yang, and C. H. Zhou, "Layered double hydroxide uniformly coated on mesoporous silica with tunable morphorlogies for catalytic transesterification of glycerol with dimethyl carbonate," *Applied Clay Science*, vol. 210, Article ID 106135, 2021.

[102] G. Liu, J. Yang, Y. Zhao, and X. Xu, "Embedded ionic liquid modified ZIF-8 in CaMgAl hydrotalcites for bio-glycerol transesterification," *RSC Advances*, vol. 12, no. 7, pp. 4408–4416, 2022.

[103] C. Len and R. Luque, "Continuous flow transformations of glycerol to valuable products: an overview," *Sustainable Chemical Processes*, vol. 2, no. 1, pp. 1–10, 2014.

[104] U. Arena, F. Ardolino, and F. Di Gregorio, "Technological, environmental and social aspects of a recycling process of post-consumer absorbent hygiene products," *Journal of Cleaner Production*, vol. 127, pp. 289–301, 2016.

[105] S. Wang, L. Xu, L. Xu, C. Tian, and Y. Guan, "Optimization of process variables in the synthesis of tributyl citrate using a polyvinylpolypyrrolidone-supported brønsted acidic ionic liquid catalyst," *International Journal of Polymer Science*, vol. 2018, Article ID 1953563, 9 pages, 2018.

[106] J. Wang, Y. Liang, S. Wang et al., "Using diaper waste to prepare magnetic catalyst for the synthesis of glycerol carbonate," *International Journal of Polymer Science*, vol. 2020, Article ID 9403714, 9 pages, 2020.

[107] P. Zhang, Y. Chen, M. Zhu et al., "Acidic–basic bifunctional magnetic mesoporous CoFe2O4@(CaO–ZnO) for the synthesis of glycerol carbonate," *Catalysis Letters*, vol. 150, no. 10, pp. 2863–2872, 2020.

[108] P. Zhang, M. Zhu, M. Fan, P. Jiang, and Y. Dong, "Rare earth-doped calcium-based magnetic catalysts for transesterification of glycerol to glycerol carbonate," *Journal of the Chinese Chemical Society*, vol. 66, no. 2, pp. 164–170, 2019.

[109] G. P. Deshmukh and G. D. Yadav, "Tuneable transesterification of glycerol with dimethyl carbonate for synthesis of glycerol carbonate and glycidol on MnO2 nanorods and efficacy of different polymorphs," *Molecular Catalysis*, vol. 515, no. 10, Article ID 111934, 2021.

[110] S. Arora, V. Gosu, V. Subbaramaiah, and T. C. Zhang, "Catalytic transesterification of glycerol with dimethyl carbonate to glycerol carbonate with Co_3O_4 nanoparticle incorporated MCM-41 derived from rice husk," *Canadian Journal of Chemical Engineering*, vol. 100, no. 8, pp. 1868–1883, 2021.

[111] G. Pradhan and Y. C. Sharma, "A greener and cheaper approach towards synthesis of glycerol carbonate from bio waste glycerol using CaO–TiO2 Nanocatalysts," *Journal of Cleaner Production*, vol. 315, no. 2, Article ID 127860, 2021.

[112] A. Devarajan, S. Thiripuranthagan, R. Radhakrishnan, and S. Kumaravel, "Solvent free transesterification of glycerol into glycerol carbonate over nanostructured CaAl hydrotalcite catalyst," *Journal of Nanoscience and Nanotechnology*, vol. 18, no. 7, pp. 4588–4599, 2018.

[113] J. Poolwong, S. Del Gobbo, and V. D'Elia, "Transesterification of dimethyl carbonate with glycerol by perovskite-based mixed metal oxide nanoparticles for the atom-efficient production of glycerol carbonate," *Journal of Industrial and Engineering Chemistry*, vol. 104, pp. 43–60, 2021.

[114] M. Tudorache, A. Negoi, B. Tudora, and V. I. Parvulescu, "Environmental-friendly strategy for biocatalytic conversion of waste glycerol to glycerol carbonate," *Applied Catalysis B: Environmental*, vol. 146, pp. 274–278, 2014.

[115] Y. Du, J. Gao, W. Kong et al., "Enzymatic synthesis of glycerol carbonate using a lipase immobilized on magnetic organosilica nanoflowers as a catalyst," *ACS Omega*, vol. 3, no. 6, pp. 6642–6650, 2018.

[116] M. A. Do Nascimento, L. E. Gotardo, R. A. C. Leão, A. M. De Castro, R. O. M. A. De Souza, and I. Itabaiana, "Enhanced productivity in glycerol carbonate synthesis under continuous flow conditions: combination of immobilized lipases from porcine pancreas and Candida Antarctica (CALB) on epoxy resins," *ACS Omega*, vol. 4, no. 1, pp. 860–869, 2019.

[117] M. Tudorache, L. Protesescu, S. Coman, and V. I. Parvulescu, "Efficient bio-conversion of glycerol to glycerol carbonate catalyzed by lipase extracted from Aspergillus Niger," *Green Chemistry*, vol. 14, no. 2, pp. 478–482, 2012.

[118] S. P. de Souza, R. A. D. de Almeida, G. G. Garcia et al., "Immobilization of lipase B from Candida Antarctica on epoxy-functionalized silica: characterization and improving biocatalytic parameters," *Journal of Chemical Technology and Biotechnology*, vol. 93, no. 1, pp. 105–111, 2018.

[119] J. Gao, Y. Wang, Y. Du et al., "Construction of biocatalytic colloidosome using lipase-containing dendritic mesoporous silica nanospheres for enhanced enzyme catalysis," *Chemical Engineering Journal*, vol. 317, pp. 175–186, 2017.

[120] P. U. Naik, L. Petitjean, K. Refes, M. Picquet, and L. Plasseraud, "Imidazolium-2-carboxylate as an efficient, expeditious and ecofriendly organocatalyst for glycerol carbonate synthesis," *Advanced Synthesis and Catalysis*, vol. 351, no. 11–12, pp. 1753–1756, 2009.

[121] P. U. Okoye, A. Z. Abdullah, and B. H. Hameed, "Glycerol carbonate synthesis from glycerol and dimethyl carbonate using trisodium phosphate," *Journal of the Taiwan Institute of Chemical Engineers*, vol. 68, pp. 51–58, 2016.

[122] S. Wang, L. Xu, P. U. Okoye, S. Li, and C. Tian, "Microwave-assisted transesterification of glycerol with dimethyl carbonate over sodium silicate catalyst in the sealed reaction system," *Energy Conversion and Management*, vol. 164, pp. 543–551, 2018.

[123] S. Wang, P. Hao, S. Li, A. Zhang, Y. Guan, and L. Zhang, "Synthesis of glycerol carbonate from glycerol and dimethyl carbonate catalyzed by calcined silicates," *Applied Catalysis A: General*, vol. 542, pp. 174–181, 2017.

[124] P. Devi, U. Das, and A. K. Dalai, "Production of glycerol carbonate using a novel Ti-SBA-15 catalyst," *Chemical Engineering Journal*, vol. 346, pp. 477–488, 2018.

[125] X. Wang, P. Zhang, P. Cui, W. Cheng, and S. Zhang, "Glycerol carbonate synthesis from glycerol and dimethyl carbonate using guanidine ionic liquids," *Chinese Journal of Chemical Engineering*, vol. 25, no. 9, pp. 1182–1186, 2017.

[126] E. Elhaj, H. Wang, and Y. Gu, "Functionalized quaternary ammonium salt ionic liquids (FQAILs) as an economic and efficient catalyst for synthesis of glycerol carbonate from glycerol and dimethyl carbonate," *Molecular Catalysis*, vol. 468, pp. 19–28, 2019.

[127] Y. Wan, Y. Lei, G. Lan, D. Liu, G. Li, and R. Bai, "Synthesis of glycerol carbonate from glycerol and dimethyl carbonate over DABCO embedded porous organic polymer as a bifunctional and robust catalyst," *Applied Catalysis A: General*, vol. 562, pp. 267–275, 2018.

[128] Y. Liu, Z. Yin, Z. Wang, R. Mou, and Z. Wei, "Synthesis of glycerol carbonate with high surface area ZrO2–KOH catalyst," *Research on Chemical Intermediates*, vol. 48, no. 6, pp. 2557–2573, 2022.

[129] A. V. Shvydko, S. A. Prihod'ko, and M. N. Timofeeva, "Synthesis of glycerol carbonate from glycerol and dimethyl carbonate using strongly basic anion-exchange styrene–divinylbenzene dowex resins," *Catalysis in Industry*, vol. 14, no. 2, pp. 181–188, 2022.

[130] Y. Yi, Y. Shen, J. Sun, B. Wang, F. Xu, and R. Sun, "Basic ionic liquids promoted the synthesis of glycerol 1, 2-carbonate from glycerol," *Chinese Journal of Catalysis*, vol. 35, no. 5, pp. 757–762, 2014.

[131] D. Guzmán-Lucero, S. Castillo-Acosta, and R. Martínez-Palou, "Glycerol carbonate synthesis using poly(1-alkyl-3-vinylimidazolium) imidazolates as catalysts," *Chemistry Select*, vol. 5, no. 43, pp. 13694–13702, 2020.

[132] F. S. H. Simanjuntak, J. S. Choi, G. Lee et al., "Synthesis of glycerol carbonate from the transesterification of dimethyl carbonate with glycerol using DABCO and DABCO-anchored Merrifield resin," *Applied Catalysis B: Environmental*, vol. 165, pp. 642–650, 2015.

[133] W. Cheng, Q. Su, J. Wang, J. Sun, and F. T. T. Ng, "Ionic liquids: the synergistic catalytic effect in the synthesis of cyclic carbonates," *Catalysts*, vol. 3, no. 4, pp. 878–901, 2013.

[134] D. W. Kim, K. A. Park, M. J. Kim, D. H. Kang, J. G. Yang, and D. W. Park, "Synthesis of glycerol carbonate from urea and glycerol using polymer-supported metal containing ionic liquid catalysts," *Applied Catalysis A: General*, vol. 473, pp. 31–40, 2014.

[135] D. W. Kim and D. W. Park, "Organic-inorganic hybrids of imidazole complexes of zinc (II) for catalysts in the glycerolysis of urea," *Journal of Nanoscience and Nanotechnology*, vol. 14, no. 6, pp. 4632–4638, 2014.

[136] S. Sahani, T. Roy, and Y. Chandra Sharma, "Clean and efficient production of biodiesel using barium cerate as a heterogeneous catalyst for the biodiesel production; kinetics and thermodynamic study," *Journal of Cleaner Production*, vol. 237, Article ID 117699, 2019.

[137] D. Singh, B. Reddy, A. Ganesh, and S. Mahajani, "Zinc/lanthanum mixed-oxide catalyst for the synthesis of glycerol carbonate by transesterification of glycerol," *Industrial & Engineering Chemistry Research*, vol. 53, no. 49, pp. 18786–18795, 2014.

[138] S. Pan, L. Zheng, R. Nie, S. Xia, P. Chen, and Z. Hou, "Transesterification of glycerol with dimethyl carbonate to glycerol carbonate over Na-based zeolites," *Chinese Journal of Catalysis*, vol. 33, no. 11-12, pp. 1772–1777, 2012.

[139] G. P. Fernandes and G. D. Yadav, "Selective glycerolysis of urea to glycerol carbonate using combustion synthesized magnesium oxide as catalyst," *Catalysis Today*, vol. 309, pp. 153–160, 2018.

[140] D. Wang, X. Zhang, X. Cong, S. Liu, and D. Zhou, "Influence of Zr on the performance of Mg-Al catalysts via hydrotalcite-like precursors for the synthesis of glycerol carbonate from urea and glycerol," *Applied Catalysis A: General*, vol. 555, pp. 36–46, 2018.

[141] D. M. Chaves and M. J. Da Silva, "A selective synthesis of glycerol carbonate from glycerol and urea over Sn(OH)2: a solid and recyclable: in situ generated catalyst," *New Journal of Chemistry*, vol. 43, no. 9, pp. 3698–3706, 2019.

[142] P. U. Okoye, A. Z. Abdullah, and B. H. Hameed, "Stabilized ladle furnace steel slag for glycerol carbonate synthesis via glycerol transesterification reaction with dimethyl carbonate," *Energy Conversion and Management*, vol. 133, pp. 477–485, 2017.

[143] P. U. Okoye and B. H. Hameed, "Review on recent progress in catalytic carboxylation and acetylation of glycerol as a byproduct of biodiesel production," *Renewable and Sustainable Energy Reviews*, vol. 53, pp. 558–574, 2016.